Transverse Instability of Megaripples

Hezi Yizhaq*, Itzhak Katra and Jasper Kok

*Institutes for Desert Research, Ben Gurion University

yiyeh@bgu.ac.il

Kavli Institute- Particle-Laden Flows in Nature

Field Observations of sand ripples and megaripples

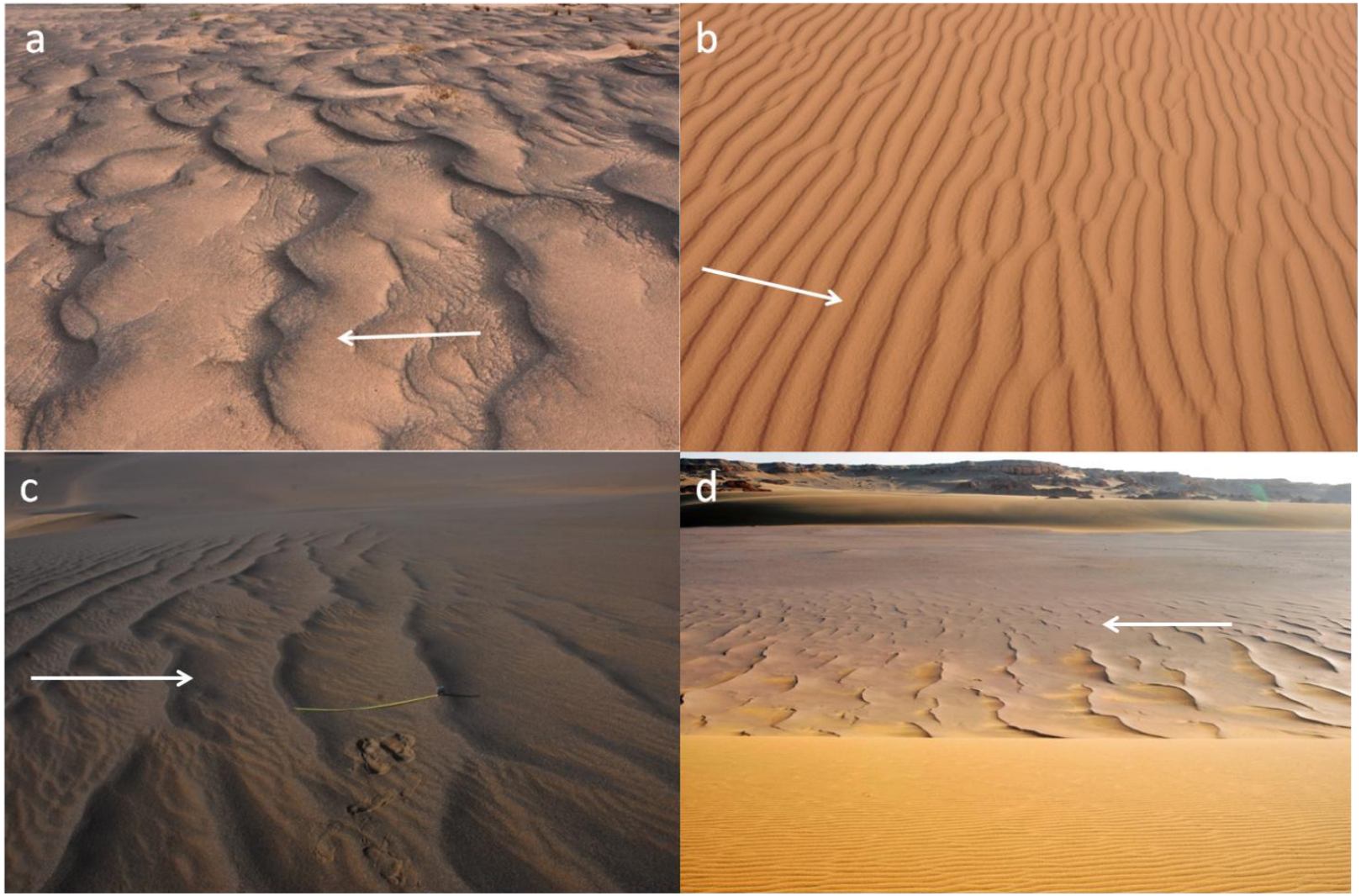

Bagnold on a giant sand ridge (Libyan Desert)

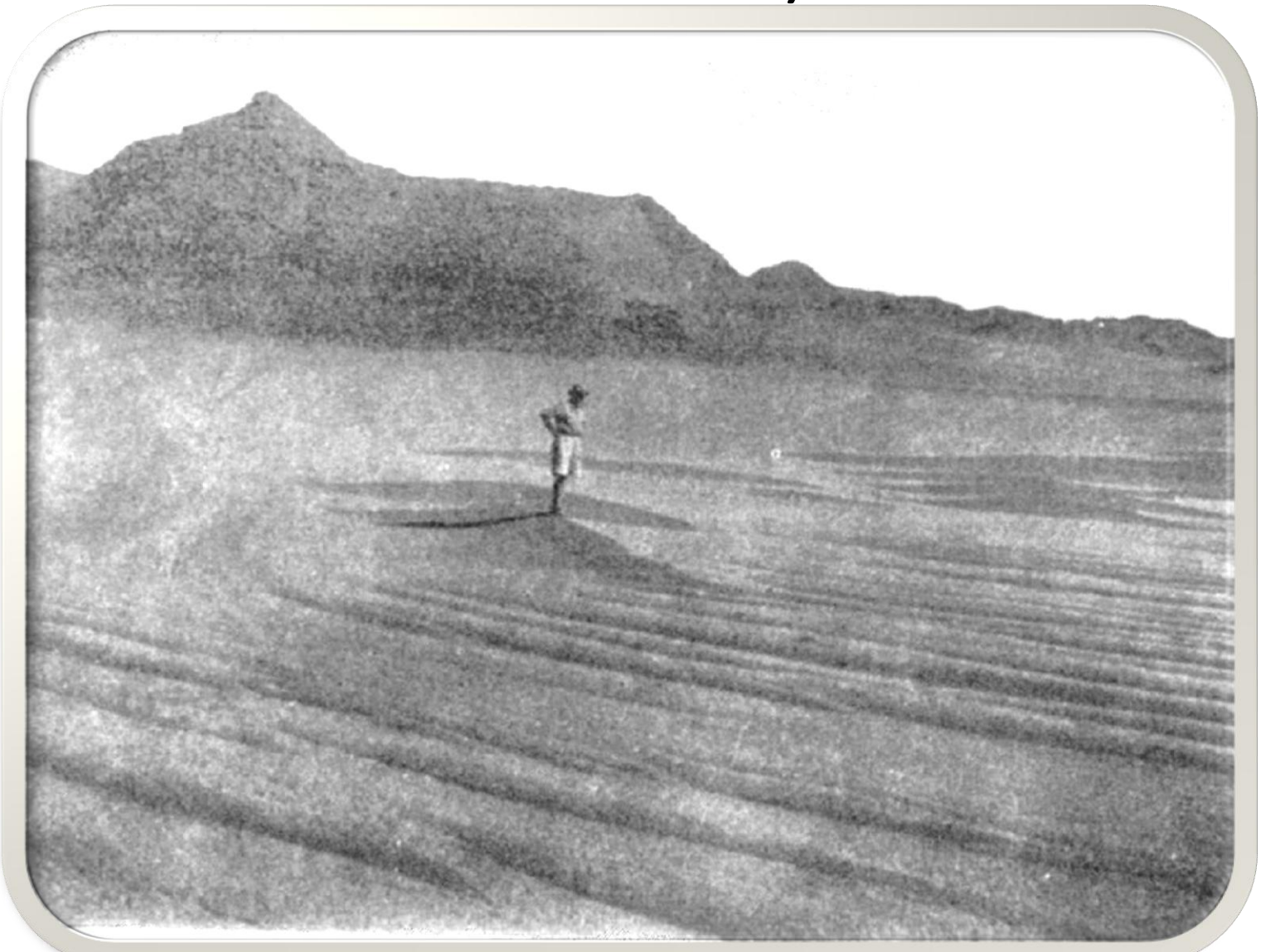

Bagnold (1941, Plate 6)

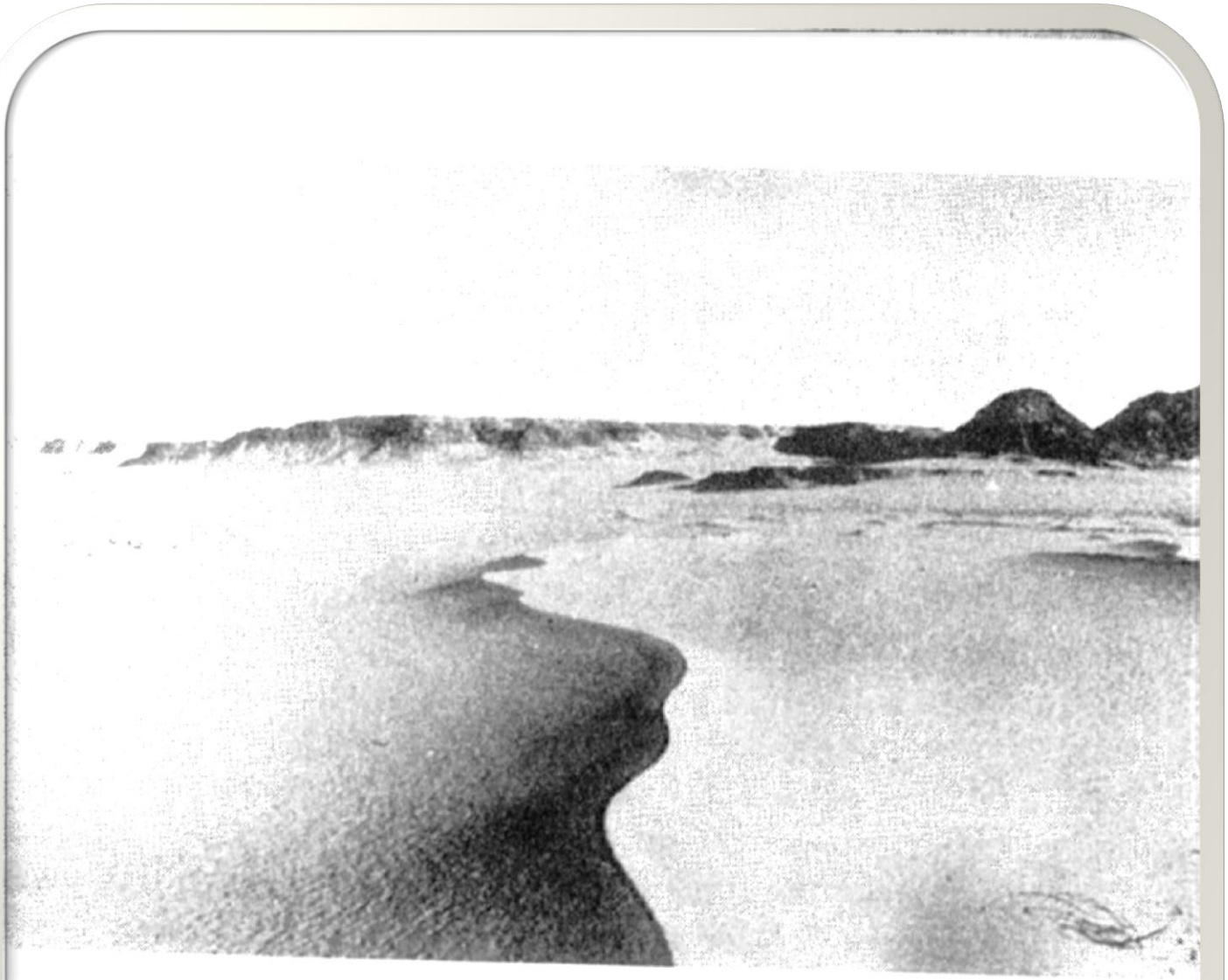

Photo R. F. Pe

GIANT SAND RIDGES (LIBYAN DESERT)

Different types of ripples at Nahal Kasuy

Edom Mountains covered by snow last week (14.12.13)

While sand ripples form almost straight lines, megaripples have greater sinuosity due to their transverse instability, a property that causes small megaripple undulations to grow with time.

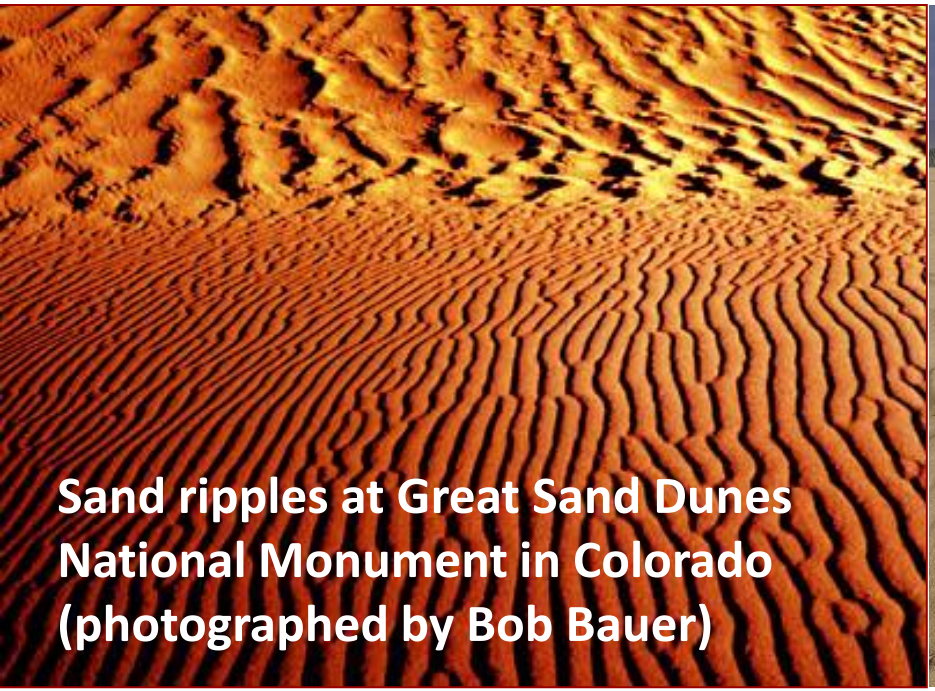

Sand ripples at Great Sand Dunes National Monument in Colorado (photographed by Bob Bauer)

Megaripples at ketura- southern IsraelPhotographed by Hezi Yizhaq

Megaripples at Grand Falls, Arizona

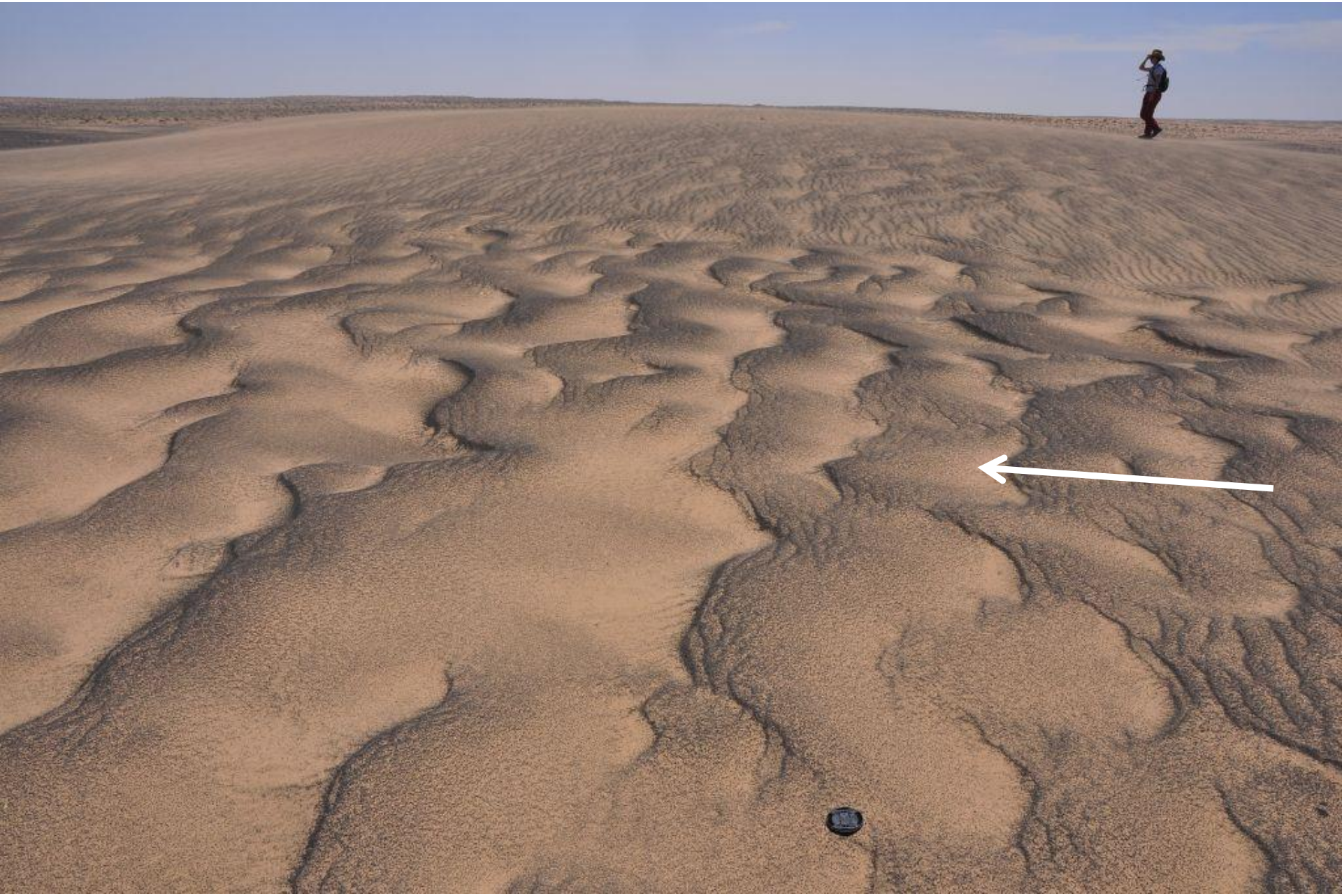

Megaripples at the Himalaya (4600 m)

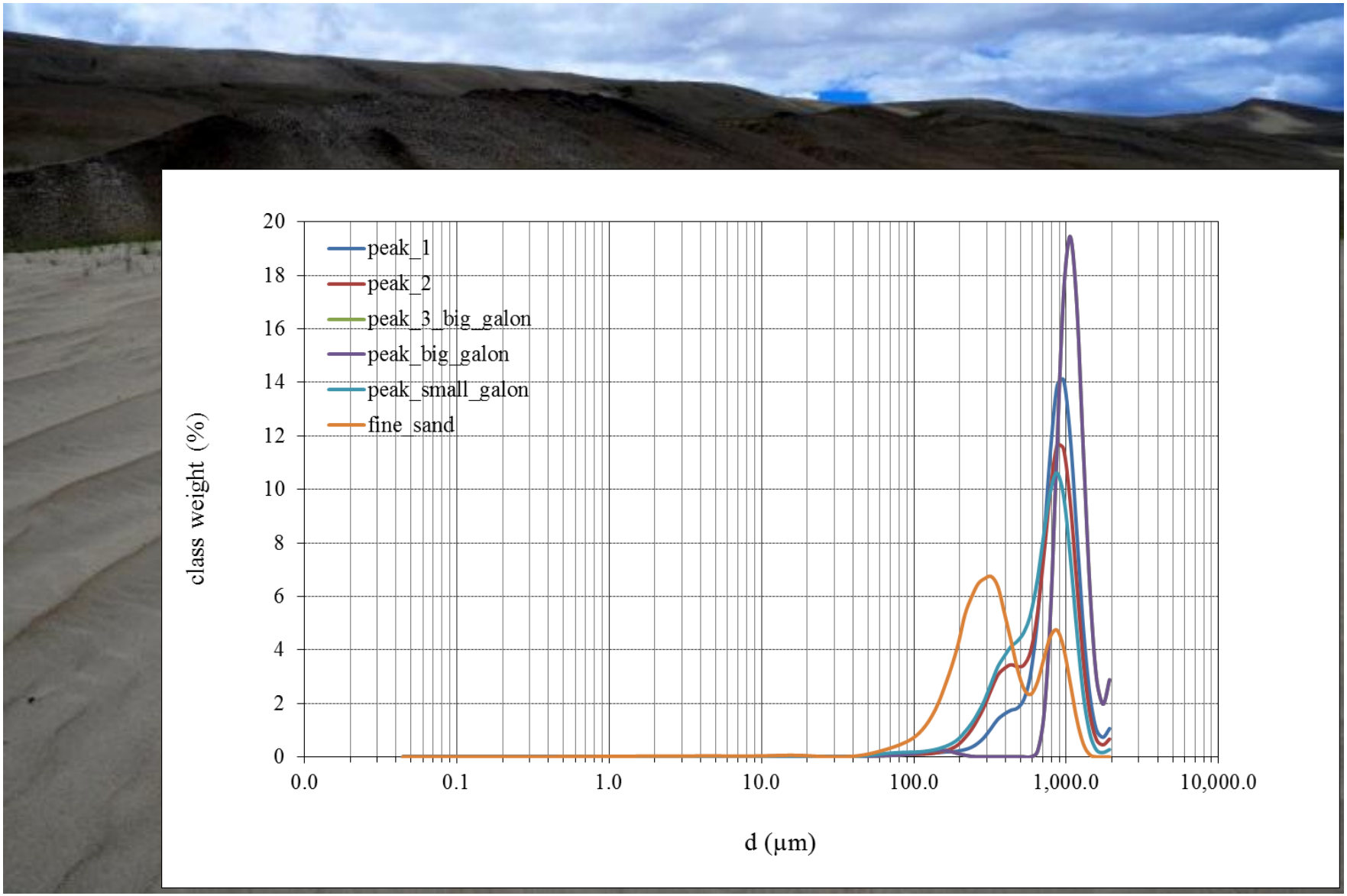

The main Questions:

- Why are sand ripples straight whereas megaripples are wavy?
- What is the mechanism behind this transverse instability of megaripples?
- How is the sinuosity of the megaripples depends on the grain size distribution?

Main features of normal ripples and megaripples

	Normal ripples	Megaripples
Wavelength	Up to	30 cm–20 m ?
Ripple index*	>15	<15
Time scale	Minutes	Days and years
Sorting	Unimodal distribution of grain sizes (typically 0.100–0.300 mm in diameter)	Bimodal distribution of grain sizes, with coarse grains 0.7–4 mm in diameter
Basic Process	Saltation and reptation (creep) of fine grains	Saltation and reptation of fine grains and creep of coarse grains.
Plan View	Crests form almost straight, continuous lines	Generally, the crests form wavy and discontinuous lines
*Ripple index = ratio of wavelength to height		

Huge megaripples (or gravel ripples) at the Puna plateau (Argentina) discovered by Juan R. Milana (2000)

Bagnold (1941, p. 149)

- "the term **ripple** has been applied to those surface forms whose wavelengths depends on the wind strength, and remains constant as time goes on; and those other forms whose wavelength may increase indefinitely with time are called **ridges**"

Megaripples morphometry according to previous studies

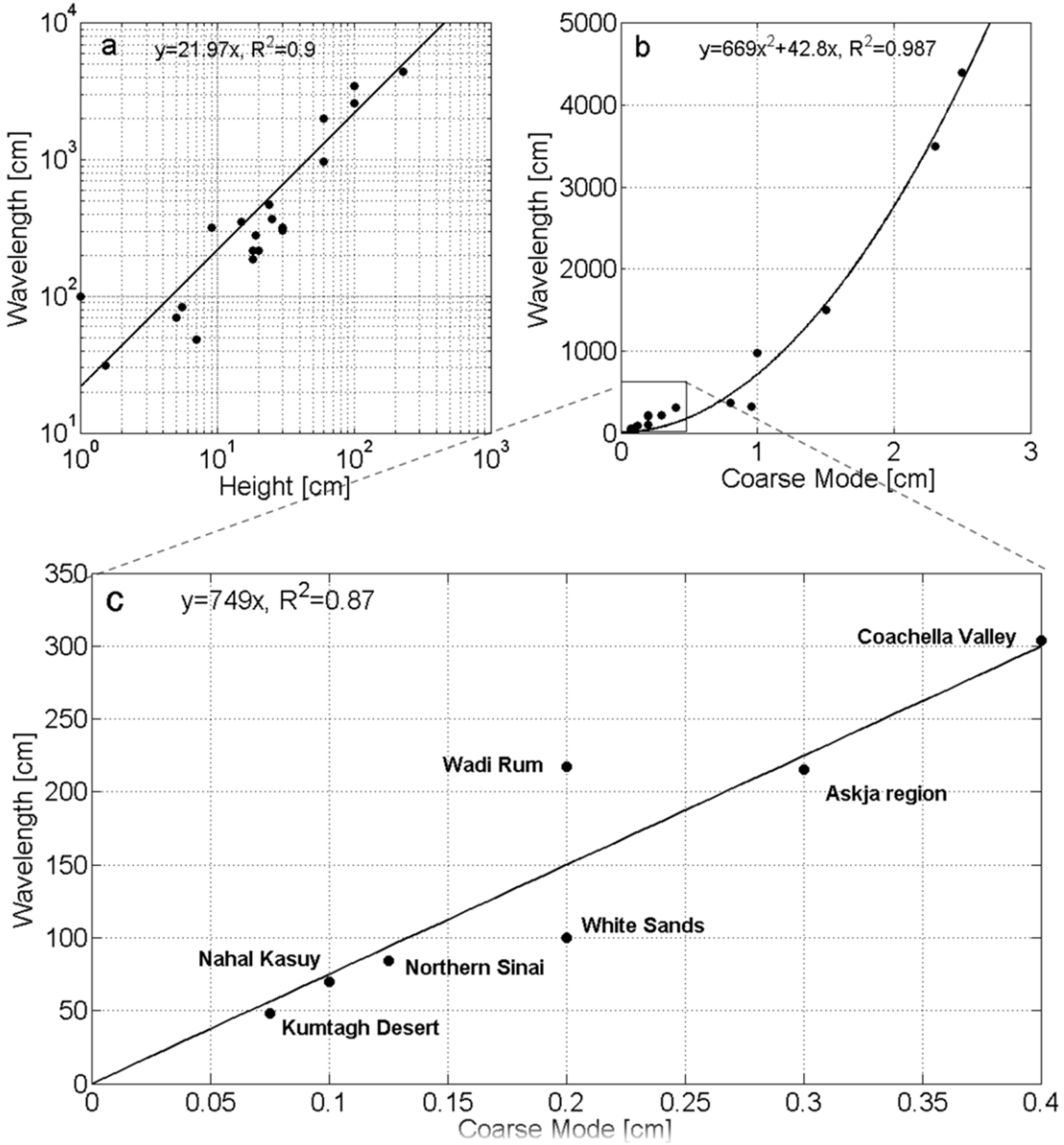

Evolution of the instability-field study

Photogrammetry

Nikon D80,

Sigma 10-20 mm

Processing with Erdas Imagine version 9.1 and its Leica Photogrammetry Software (LPS) extension

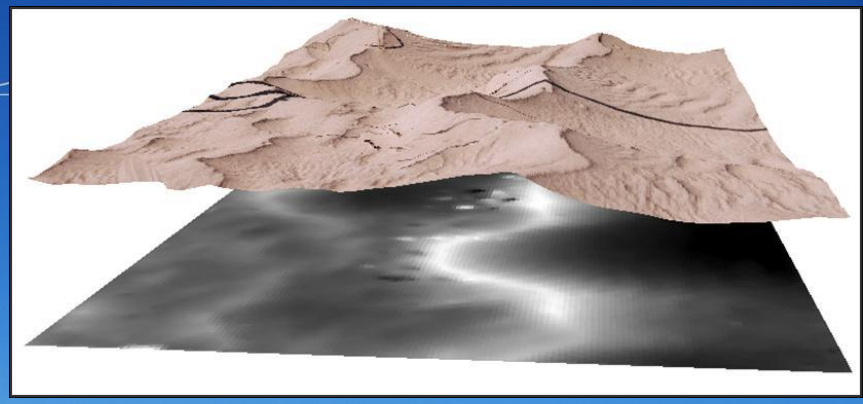

Digital Elevation Model (DEM

To avoid interfering with plot dynamics, the imaging and the ground control point (GCP) markings had to be made from outside.

Method 1: Iron rods

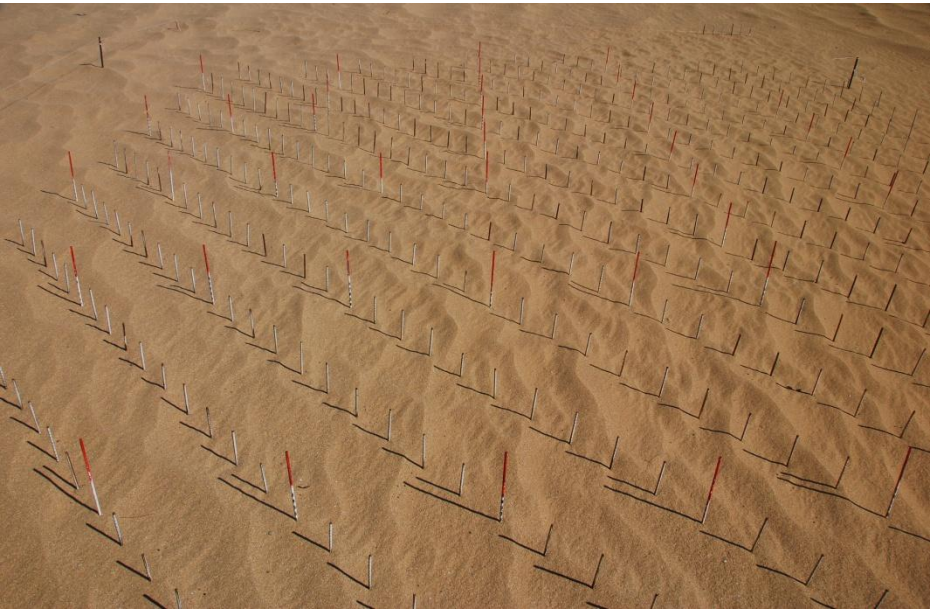

0.6 mm in diameter and 12 cm in height above the surface, 15 cm horizontal spacing

Method 1: Marking holes with “giant comb” (15 cm)

The coarse particles (96% Calcite)

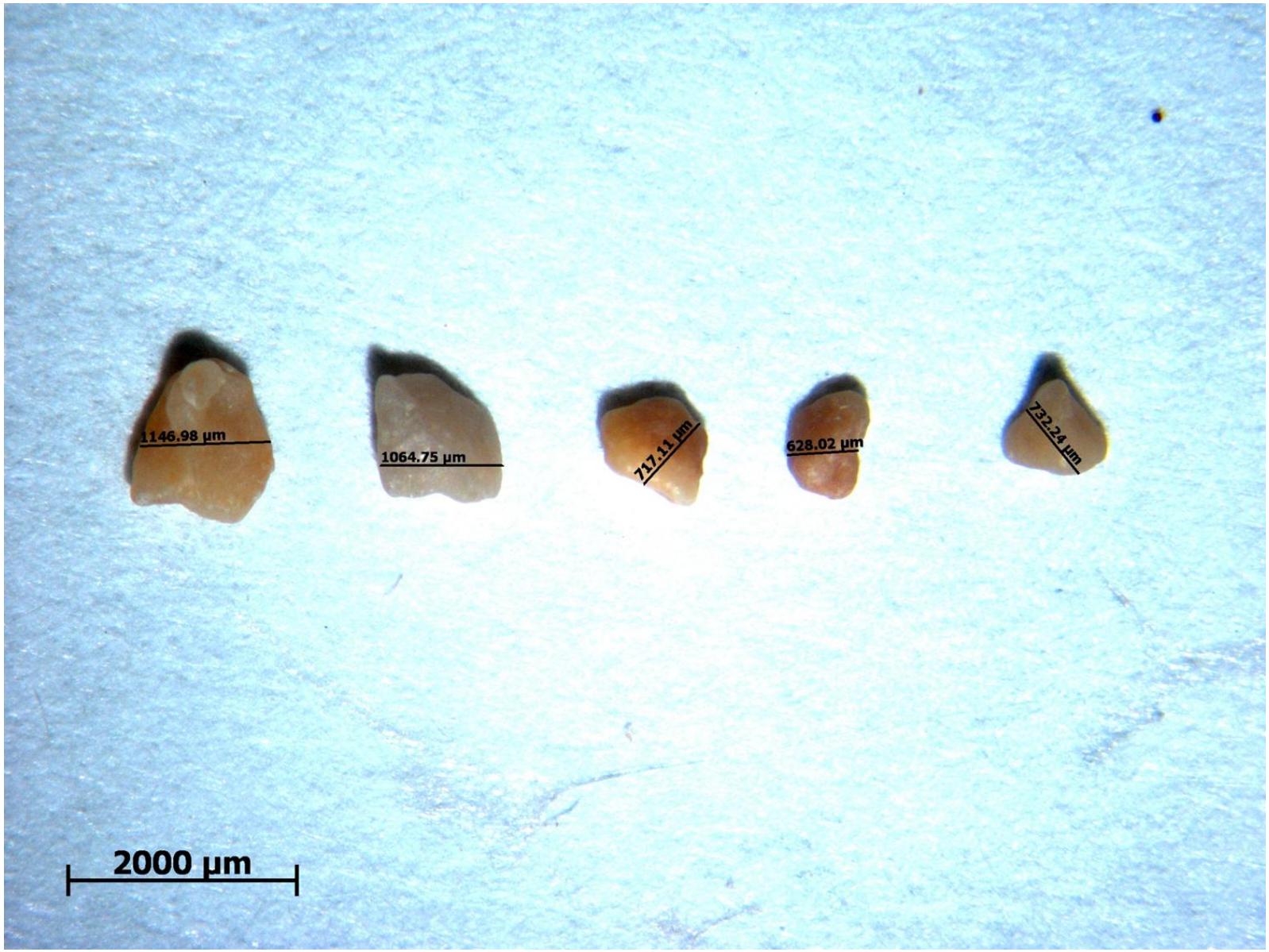

Evolution of the instability-field study

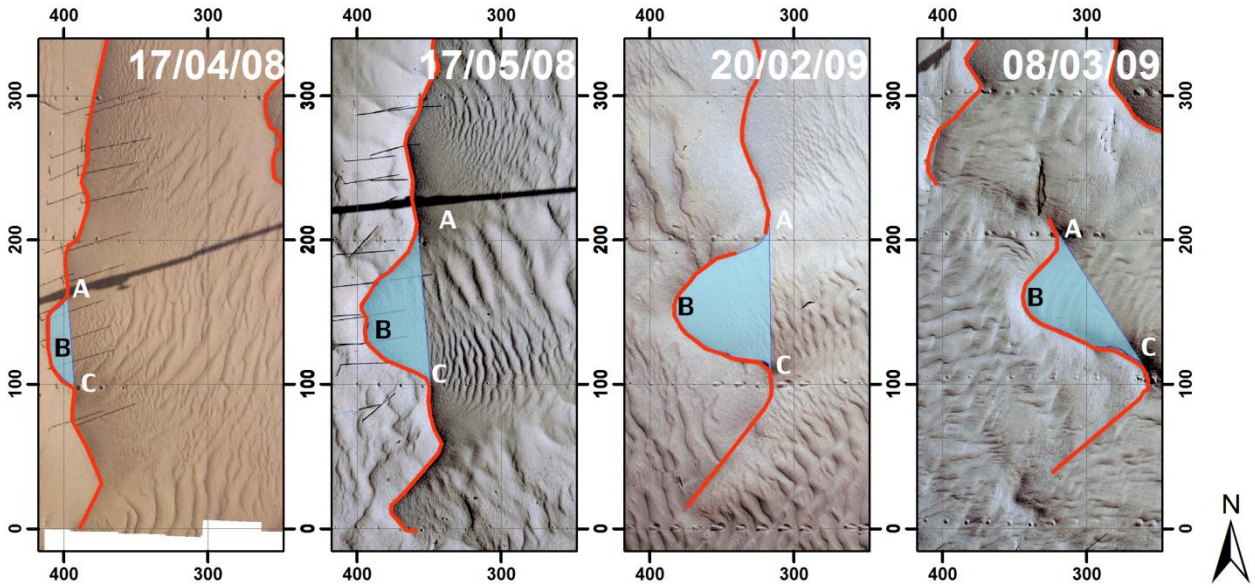

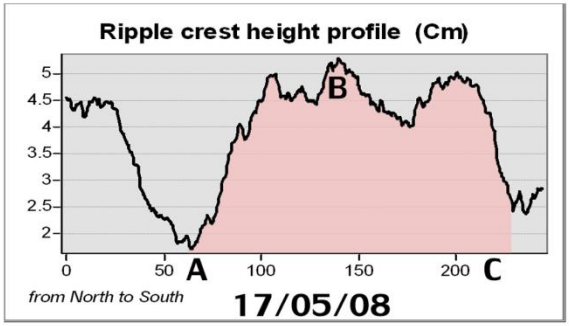

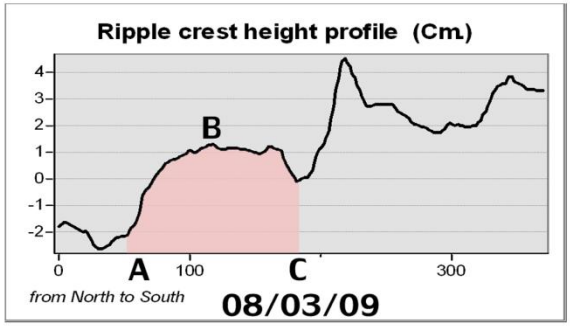

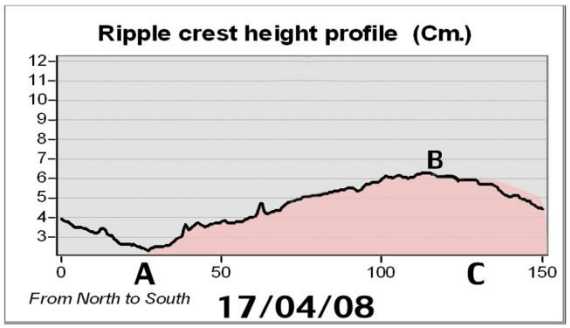

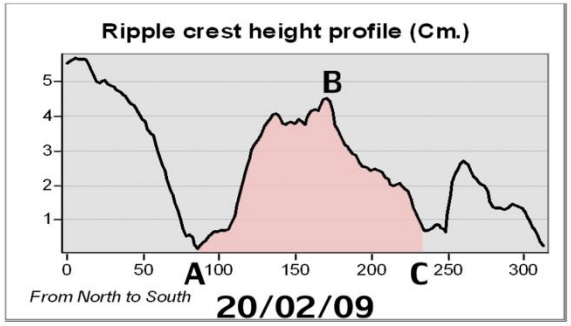

Size parameters of the megaripple during the period 17/4/08-8/3/09

Date	Bay's Width [cm]	Bay's vertex Movement [cm]	Bay's Average Edges Movement [cm]	Bay's Area [cm^2]
17/4/2008	73			782
18/4-17/5/2008	108	19	44	2798
18/5/2008 - 20/2/2009	101	14	24	4055
21/2-8/3/2009	112	38	55	2831

Wind data from Nahal Kasuy

Period	DP [v.u]	RDP [v.u.]	RDD [Deg]	RDP/DP	t[%]
17/4-17/5/2008	5.34	5.18	279	0.94	7.1
18/5/2008-20/2/2008	15.97	7.28	225	0.46	7.38
21/2-8/3-2009	12.99	10.85	251	0.83	18.2

Note: DP is the drift potential; RDP is resultant drift potential; RDD is RDP direction; RDP/DP is the wind directionality and t is the time (in percent) that the wind is above the fluid threshold for sand transport (taken as 6 m/s).

$$q_c = (1-p)\rho c \frac{H}{2}$$

Basic Hypothesis (Yizhaq et al., 2012)

- The origin of the instability is due to variations in megaripple height, which do not diminish over time, and due to the inverse dependence of ripple drift velocity on the height.
- Non-uniform megaripple height may be due to irregularities in the accumulation of coarse particles (both number and sizes)
- The lateral coupling (by lateral reptation flux) in megaripples is smaller than in normal ripples

Growth of the transverse instability

$$\frac{\Delta x}{\Delta t} = c_1 - c_2 = \frac{2q_c(H_2 - H_1)}{(1-p)\rho H_1 H_2}$$

c_1, c_2 migration speeds

H_1 height of edges

H_2 height of vertex

q_c reptation flux

p porosity

ρ grain density

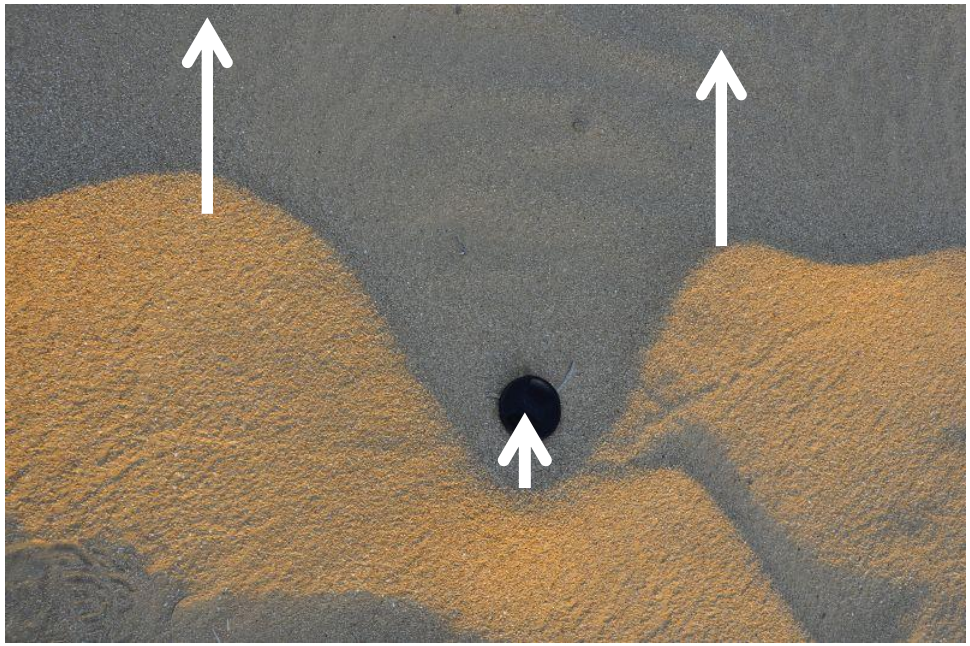

$$q_c = (1-p)\rho c \frac{H}{2}$$

Zimbelman et al., 2009

Estimation of Δx for the period 21 February – 8 March

$q_c = 9.49 \cdot 10^{-6}\ \mathrm{kg} \cdot \mathrm{m}^{-2} \cdot s^{-1}$

$p = 0.35$

$\rho = 2710\ \mathrm{kg/m}^3$

$H_1 = 0.04\ \mathrm{m}$

$H_2 = 0.08\ \mathrm{m}$

$\Delta t = 18\ \mathrm{days} \Rightarrow \Delta x = 18.62\ \mathrm{cm}$ compare to measured 17 cm

Reptation flux –COMSALT (Kok and Renno, 2009) simulations

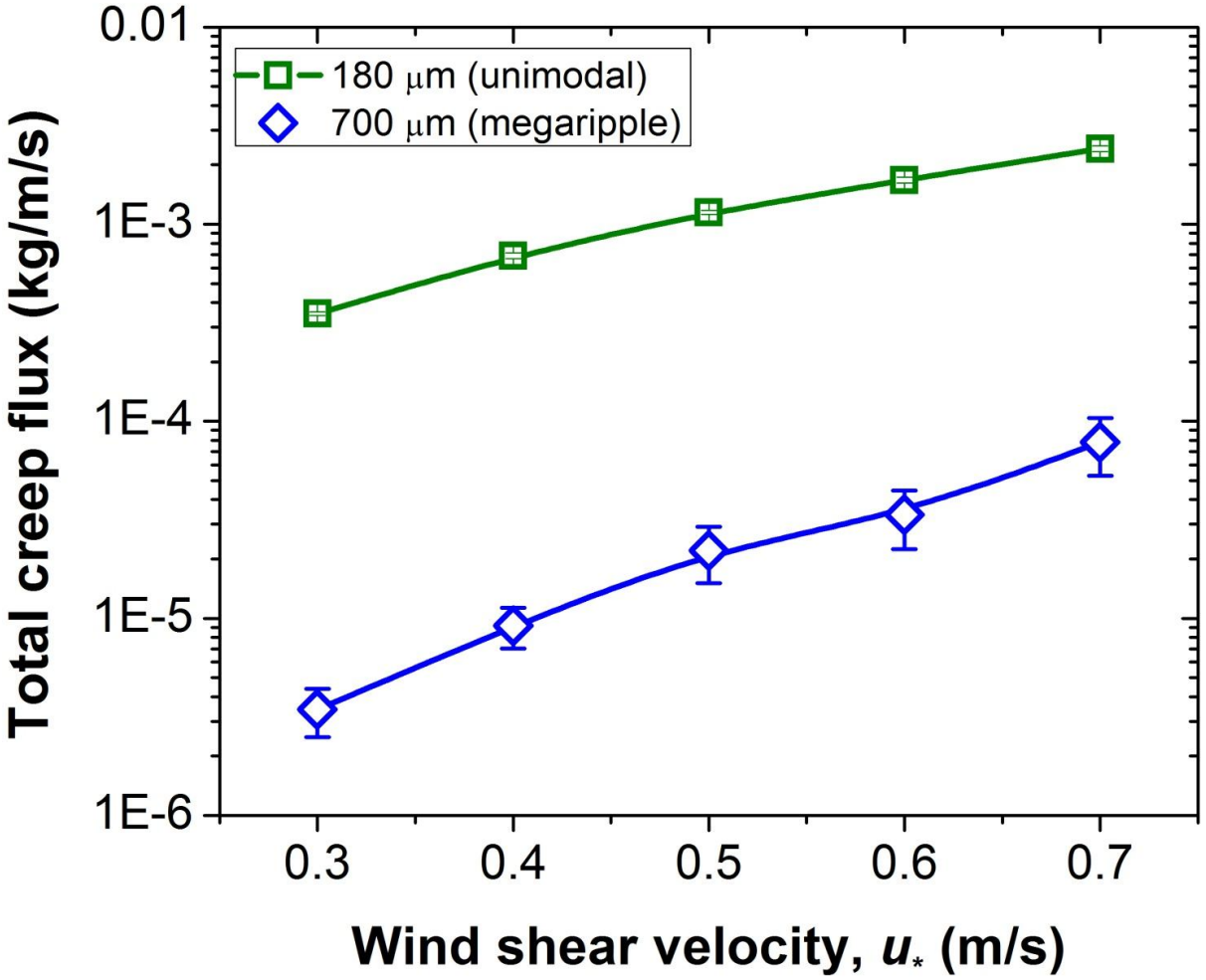

A model for sand ripples based on Anderson model (1987)

$$(1-\lambda_p)\rho\frac{\partial\zeta}{\partial t}=-\frac{\partial Q}{\partial x}$$

$\frac{\partial Q}{\partial x}>0$ Erosion

$\frac{\partial Q}{\partial x}<0$ Deposition

- λ_p porosity of the bed (about 0.35)
- ρ density of sand
- ζ elevation of the sand surface
- Q flux of sand grains

Number density of impacting grains

$$N_{im}(x) = N_{im}^{0}\left(1+\frac{\tan\theta}{\tan\phi}\right)\cos\theta$$

$$= N_{im}^{0}\cot\phi\ \frac{\tan\phi+\zeta_x}{\sqrt{1+\zeta_x^2}}$$

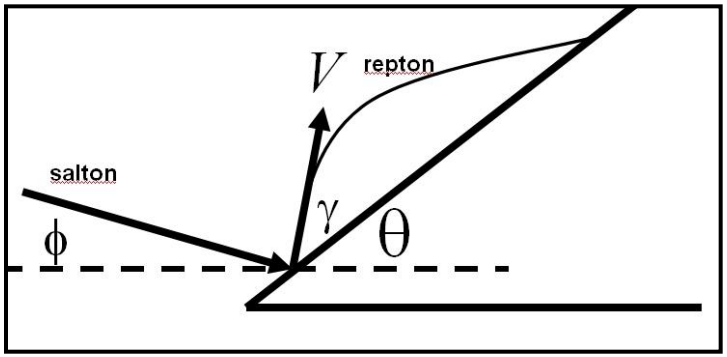

N_{im}^{0} number density of impacting grains on a horizontal surface (about 10^7 m^{-2} s^{-1})

θ inclination of the surface

$tan\ \theta = \zeta_x$

A flux correction term

- $Q_r(x,t) = Q_r^{flat}(x,t)\ (\ 1 - \mu\ \zeta_x\ )$

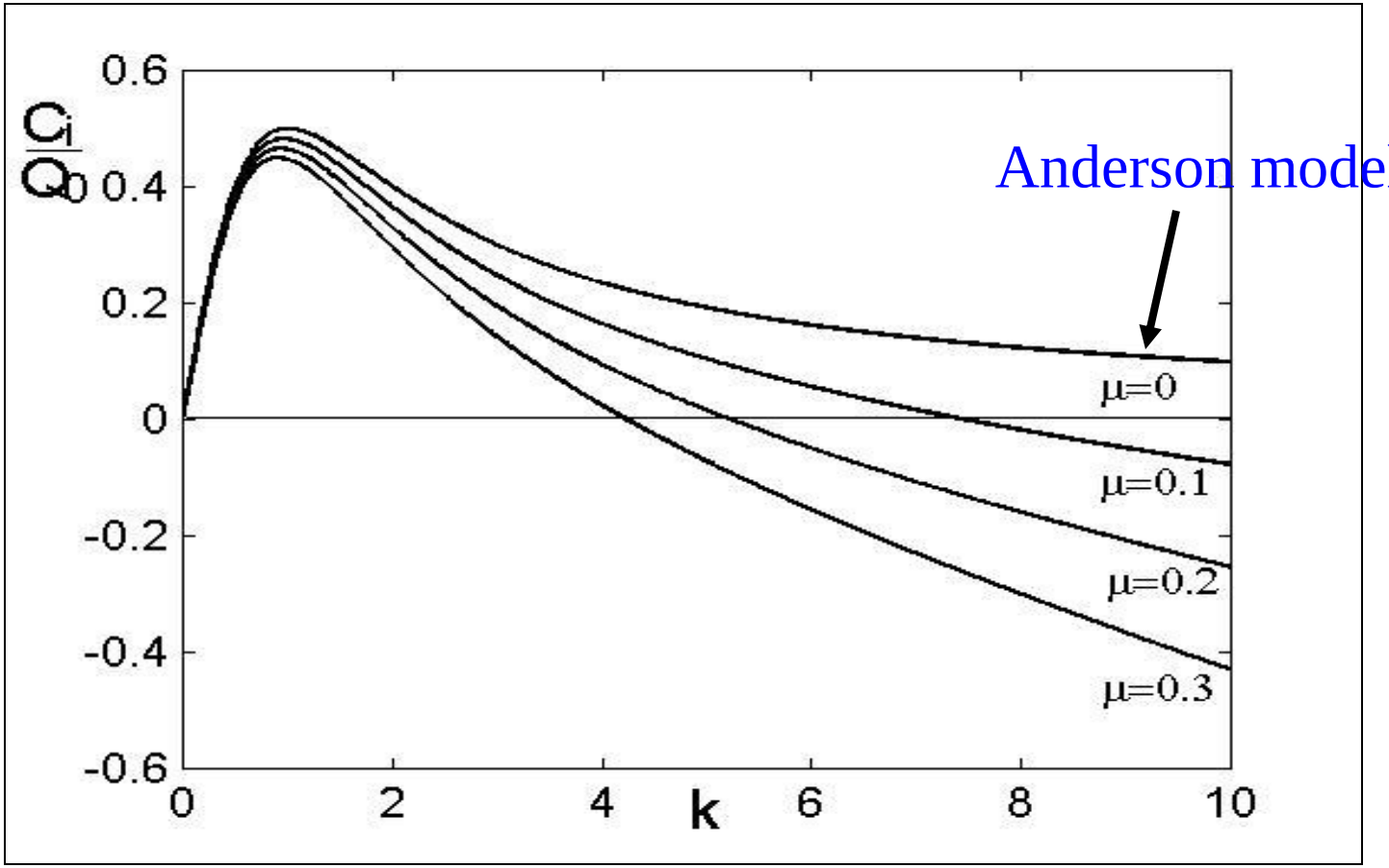

The full integral model for sand ripples

(Yizhaq, H, N.J. Balmforth and A. Provenzale) Physica D, 195, 207-228 (2004), running for martian conditions (Yizhaq et al., 2014)

$$\frac{\partial \zeta}{\partial t} = -Q_0 \frac{\partial}{\partial x}\left[(1-\mu\zeta_x) \int_{-\infty}^{\infty} d\alpha \; p(\alpha) \int_{x-\alpha}^{x} F(x')\, dx' \right]$$

$$F(x) = \mathrm{Max}\left\{ \frac{\tan\phi + \zeta_x}{\sqrt{1+\zeta_x^2}}, 0 \right\}$$

$$Q_0 = \frac{m N_r N_{im}^0 \cot\phi}{\rho(1-n)}$$

2D rippls (parameter values are given by COMSALT)

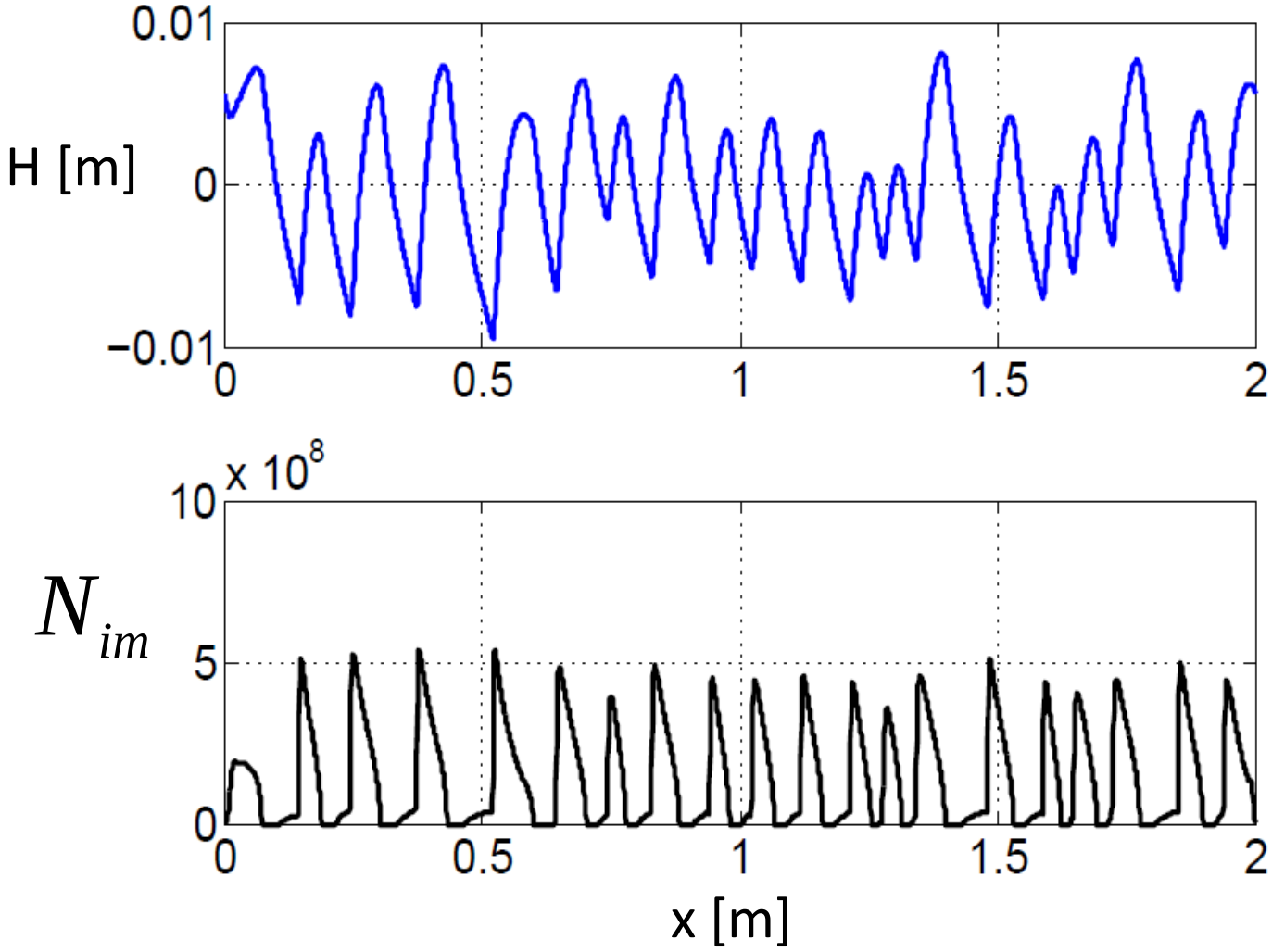

$u_* = 0.5$ m/s

Long-Wave Approximation

Goal:

Derving a compact or minimal description of the dynamics (from integro-deifferential equation to PDE) .

I. Nondimensional Variables:

$$\tilde{x} = \frac{x}{\bar{a}};\ \tilde{\alpha} = \frac{\alpha}{\bar{a}};\ \tilde{\zeta} = \frac{\zeta}{\bar{a}};\ \tilde{t} = \frac{Q_0 t}{\bar{a}};\ \tilde{p}(\tilde{\alpha}) = \bar{a}\, p(\alpha)$$

II. Near the instability onset: $\zeta(x,t) = \varepsilon\,\zeta(X,t),\ X = \varepsilon\, x$

III. Taylor series expansion of $F(X)$ and $F(X - \varepsilon\alpha)$

IV. Assuming $\mu \sim \varepsilon$ and $T = \varepsilon^2 t$; define: $\overline{a^p} = \int_{-\infty}^{\infty} \alpha^p\, p(\alpha)\, d\alpha$

Three Dimensional Ripples mathematical model : long-wave expansion equation

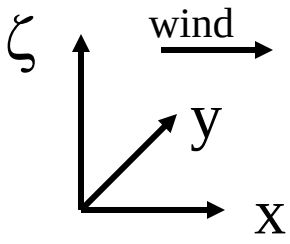

In the lateral direction we assume only rolling.

$$\zeta_t = -\partial_x Q_x - \partial_y Q_y$$

$$Q_x = Q_r^0(1-\mu\zeta_x) \qquad Q_y = -\varepsilon Q_r^0 \zeta_y$$

$$\zeta(X,Y,T)_T = -(1-\mu\tan\varphi)\zeta_{XX} + \varepsilon\tan\varphi\zeta_{YY}$$
$$+\frac{\varepsilon}{2}\left[\overline{a^2}\zeta_{XXX} + (\tan\varphi + 2\mu)(\zeta_X^2)_X\right]$$
$$+\frac{\varepsilon^2}{2}\left[-\frac{\overline{a^3}}{3}\zeta_{XXXX} + (\zeta_X^3)_X - \frac{\overline{a^2}\tan\varphi}{2}(\zeta_X^2)_{XX}\right]$$

*Yizhaq et al., Physica D, 2004

3D simulation of normal sand ripples (long-wave approximation)

$\varepsilon=\mu=0.2$
$\phi=10^0$

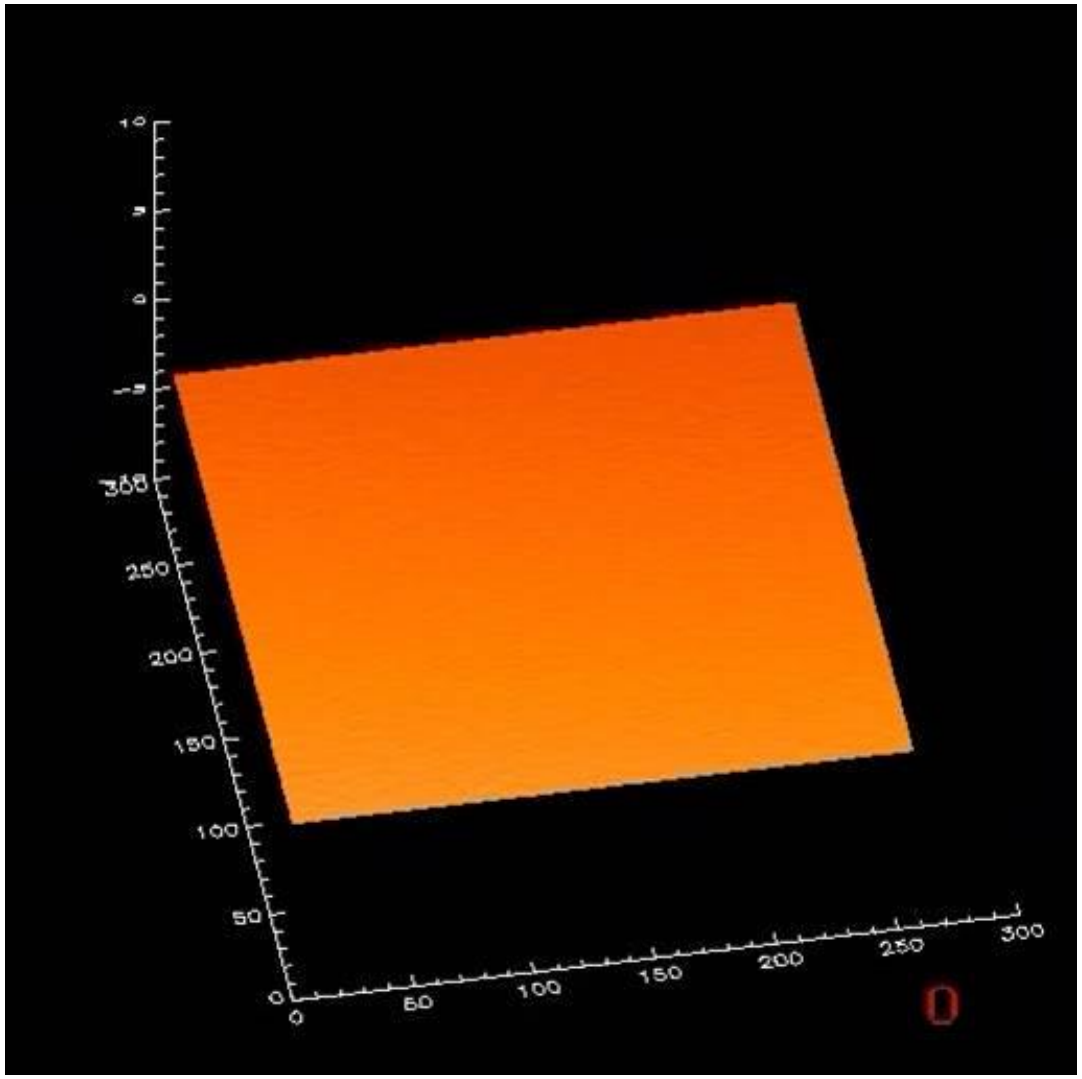

3DNormal ripples numerical simulation

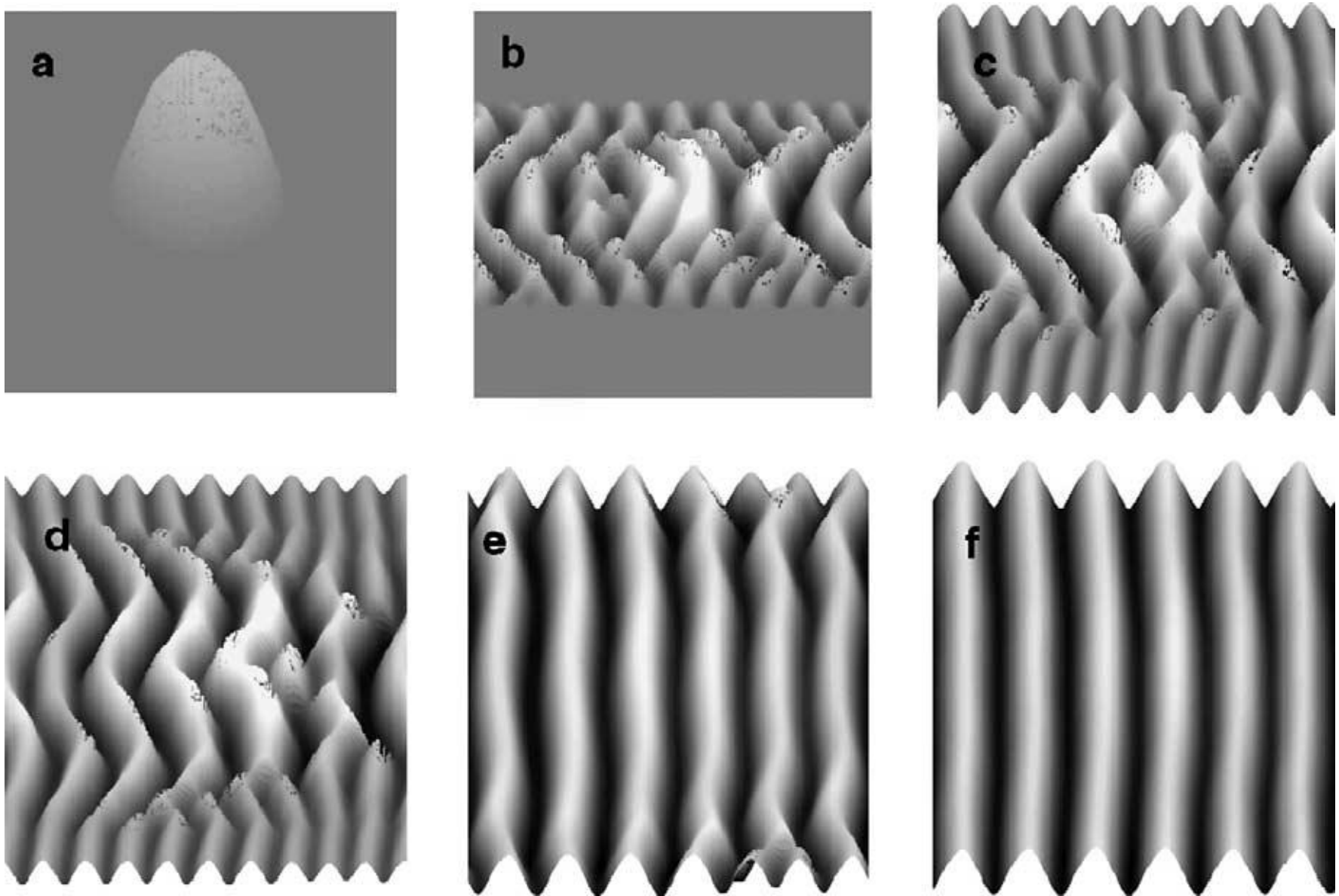

Straightness requires along-crest coupling (Rubin, 2012)

Two-dimensional bedforms and their origins:

- Longitudinal and oblique bedforms in unidirectional flows Flow and transport have an along-crest component.
- Bedforms migrating along a slope (inclined crests) gravity drives along-crest transport.
- Wind ripples along-crest transport caused by ballistic impacts that splash grains laterally.
- Bedforms in reversing flows Flow reversals reduce net across-crest transport, but allow along-crest transport.

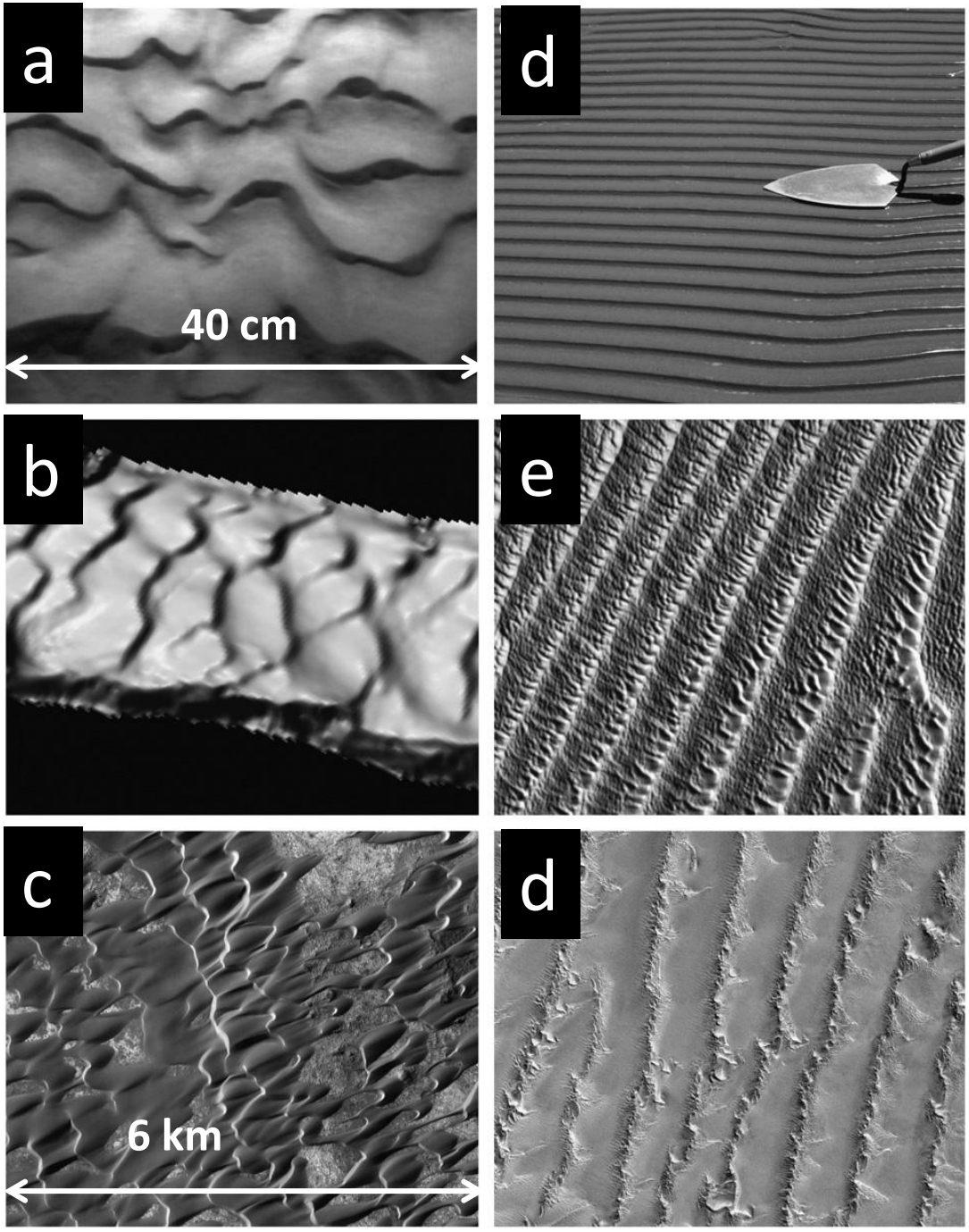

Three-dimensional ripples and dunes in unidirectional flows (left column a–c) and two-dimensional ripples and dunes in reversing flows (right column d–f). (a) Ripples formed by unidirectional flow in a lab flume; flow is from top to bottom; (b) Dunes in unidirectional flow in the Colorado River in Grand Canyon viewed by multi beam sonar (Kaplinski et al., 2009); channel width is approximately 70 m. (c) Crescentic eolian dunes on Mars (winds roughly from right to left;); (d) Ripples formed by reversing wave-generated flow on a sand bar in Colorado River in Grand Canyon. (e) Dunes formed by reversing tidal currents, San Francisco Bay, California (Barnard et al., 2011); wavelength is 60 m. (f) Eolian dunes formed by seasonally reversing winds, Namib Desert; dune wavelength is 2 km.

Wind Tunnel Experiments (Ben Gurion University)

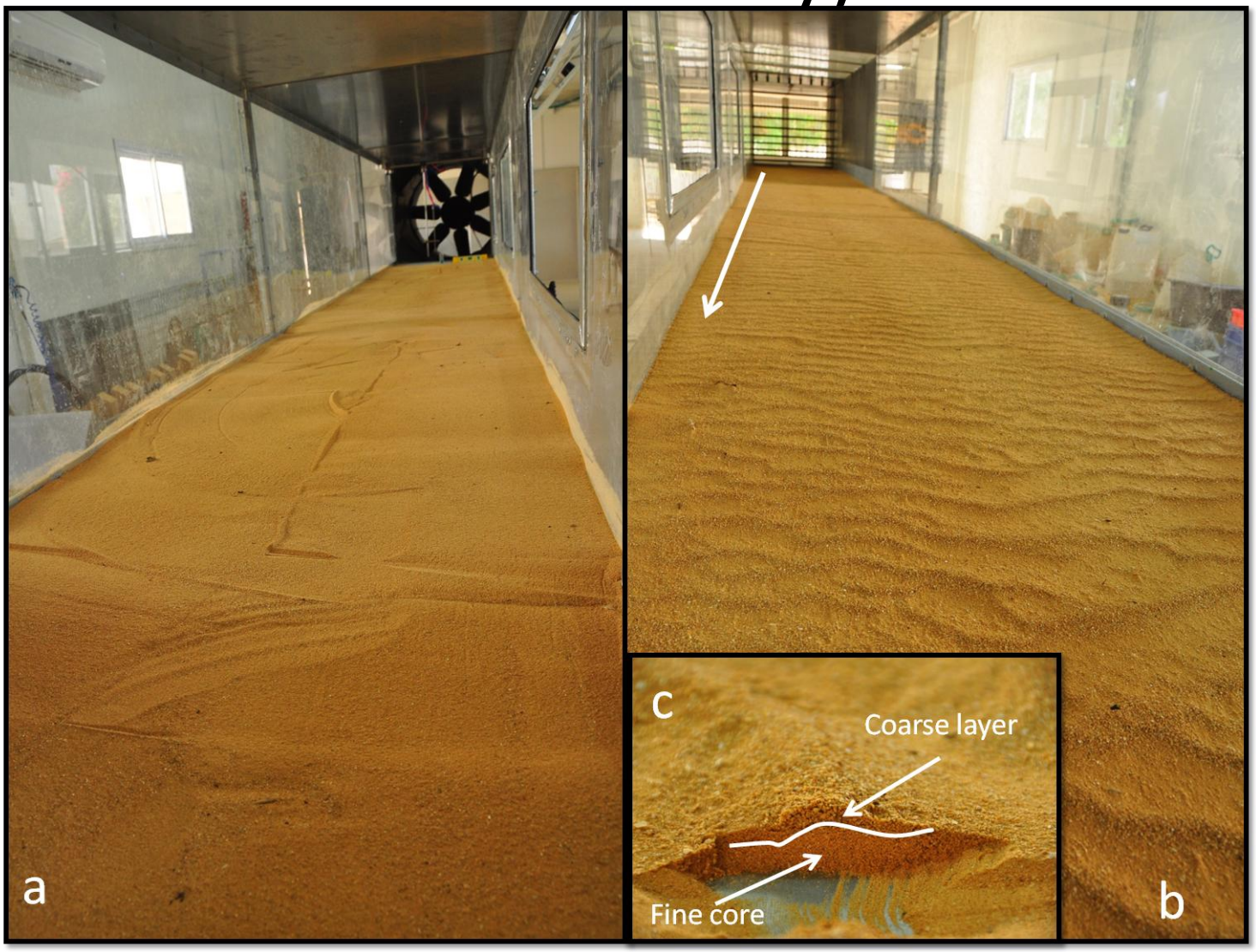

Wind tunnel Experiment with bimodal sand distribution

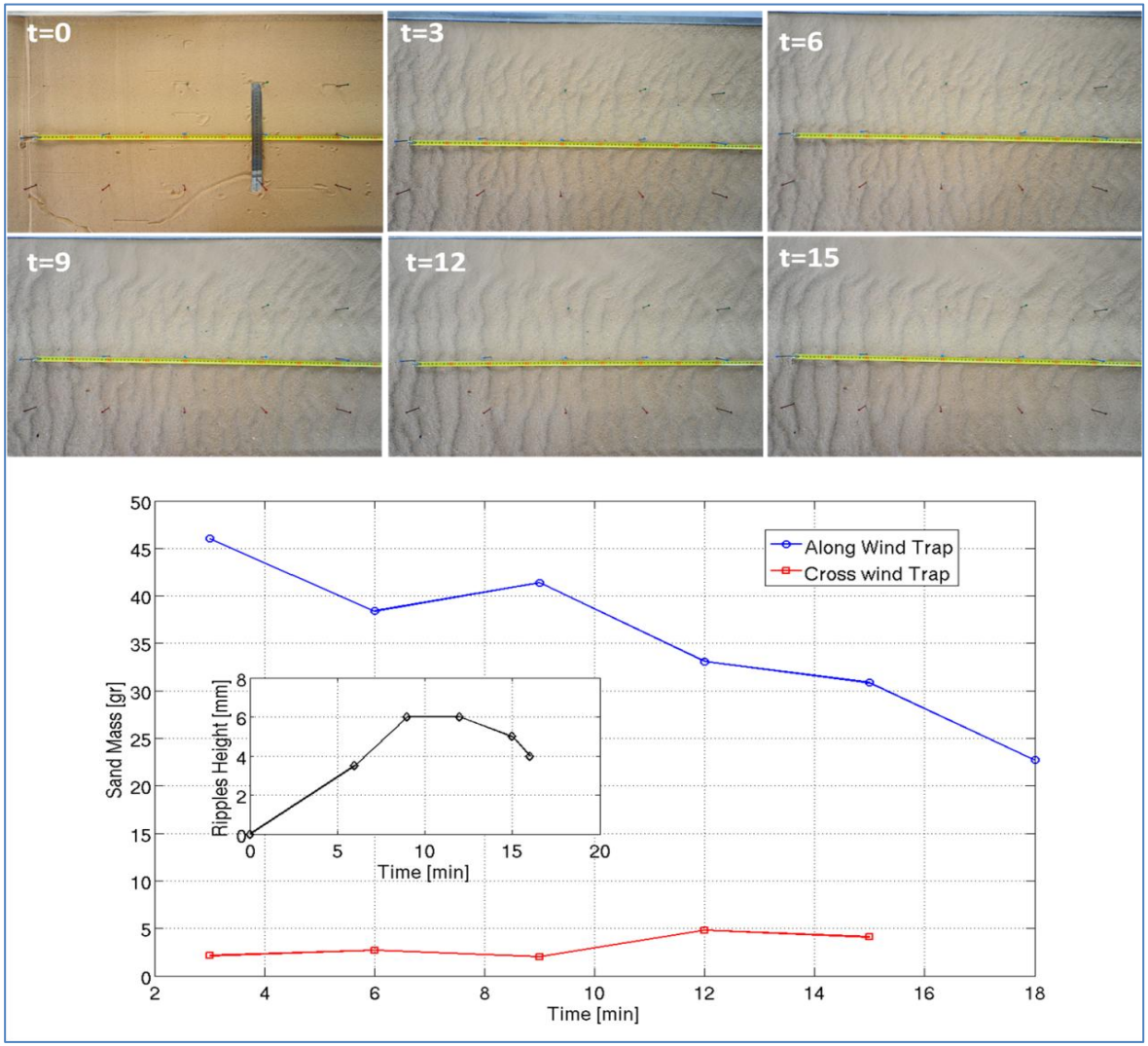

Time evolution of incipient megaripples in the wind tunnel (wind speed 7 m/s) with natural sand collected from Nahal kasuy (time measured in minutes). The bottom graph shows the mass of reptating sand collected in both directions (parallel and transverse to wind direction). The mass in the trap along the wind direction is at least four times larger than that in the cross-wind direction. The inset shows the ripple height (in mm) during the experiment.

Grain size distribution of reptation for different wind speeds

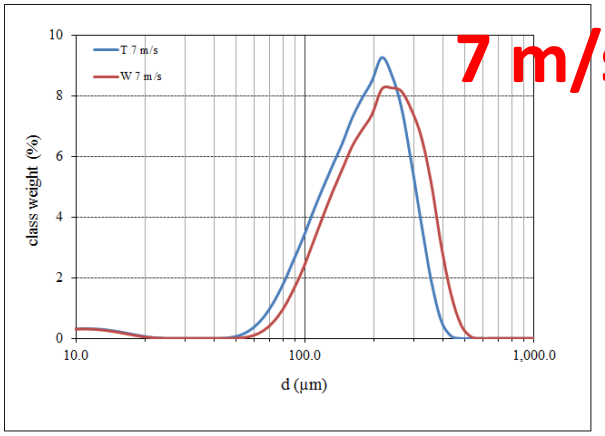

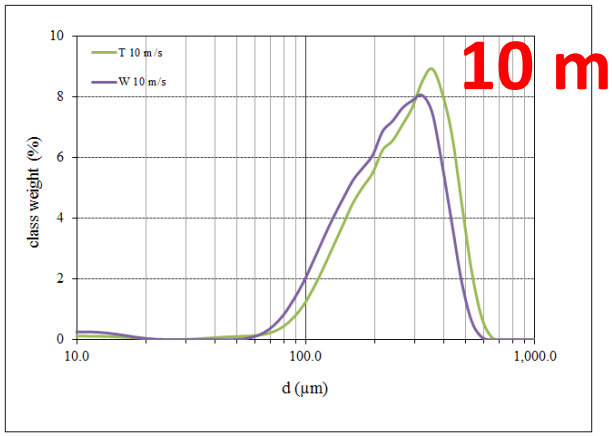

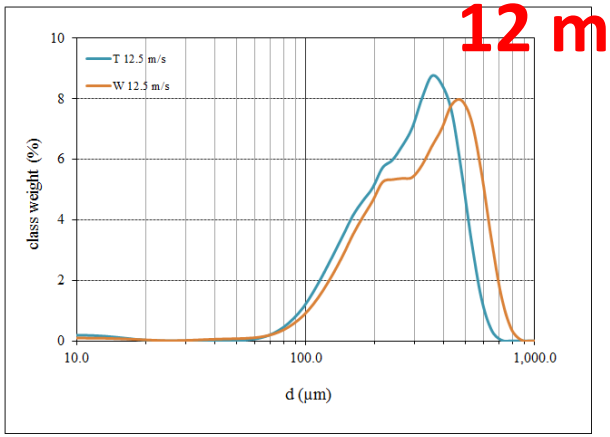

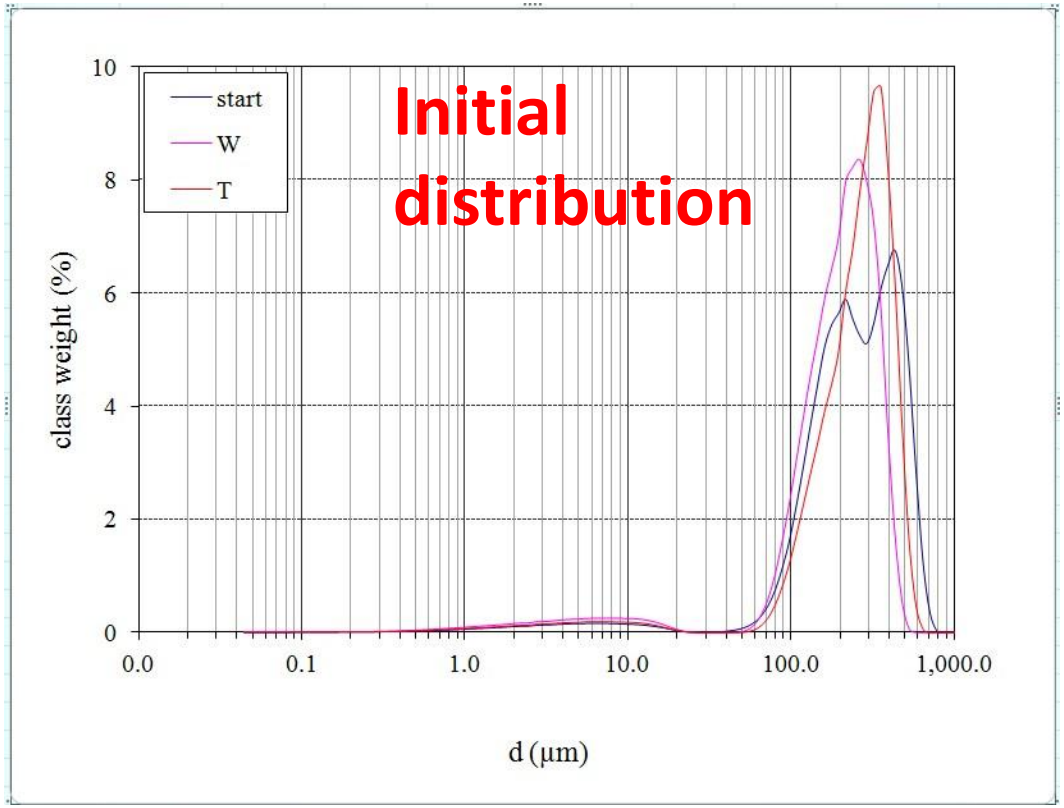

Bagnold's Explanation for the transverse instability of normal ripples (Bagnold 1941, p.161)

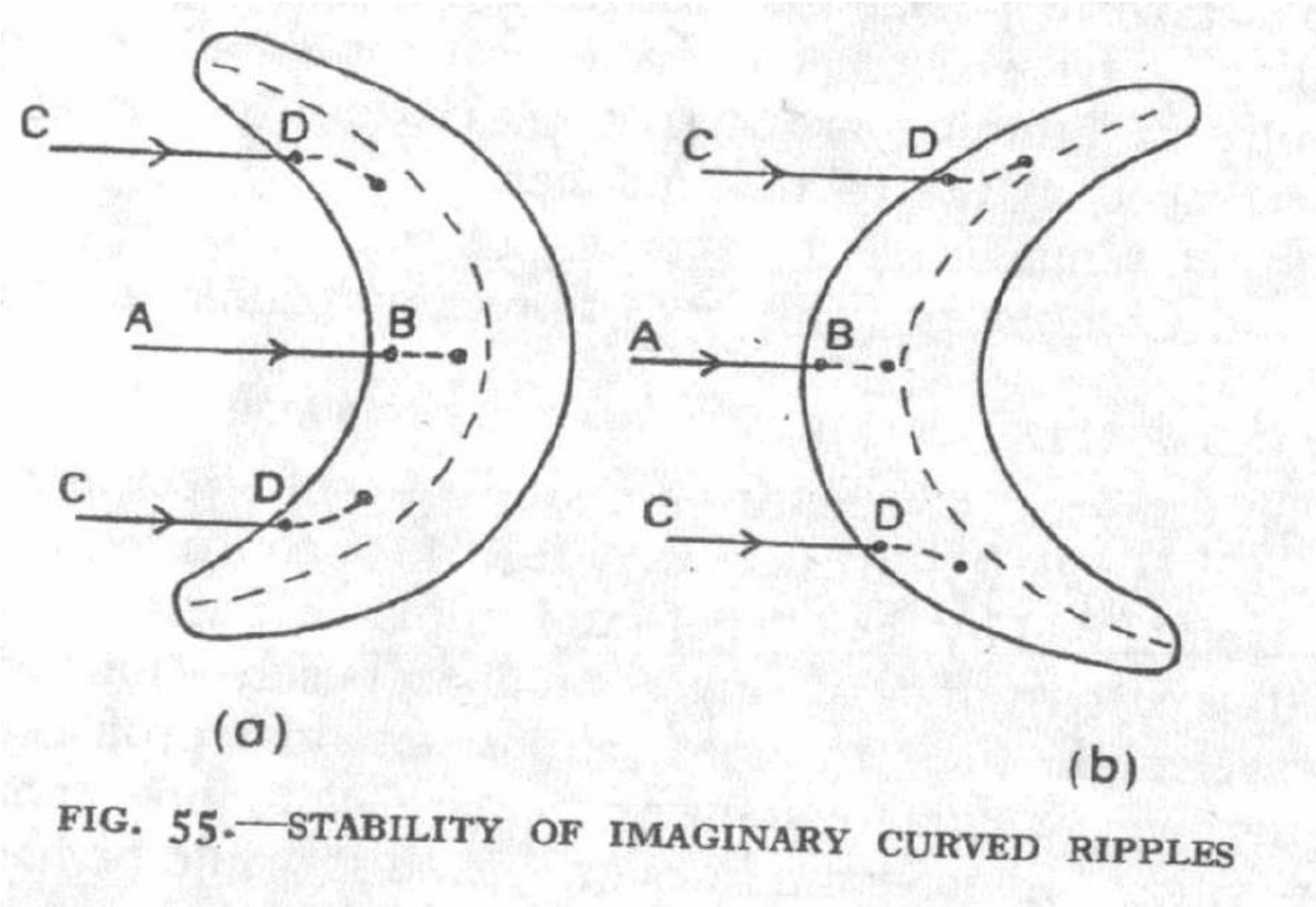

FIG. 55.—STABILITY OF IMAGINARY CURVED RIPPLES

Bagnold's Explanation

- "In ripple (a) the grains roll inwards towards the more transverse portion, and tend to accumulate there. This causes the rate of advance of the transverse portion to become slower than that of the oblique portion."
- The above explanation, though simple, is at present merely tentative".

The four suggested basic dynamics of curved section of the ripple (top view)

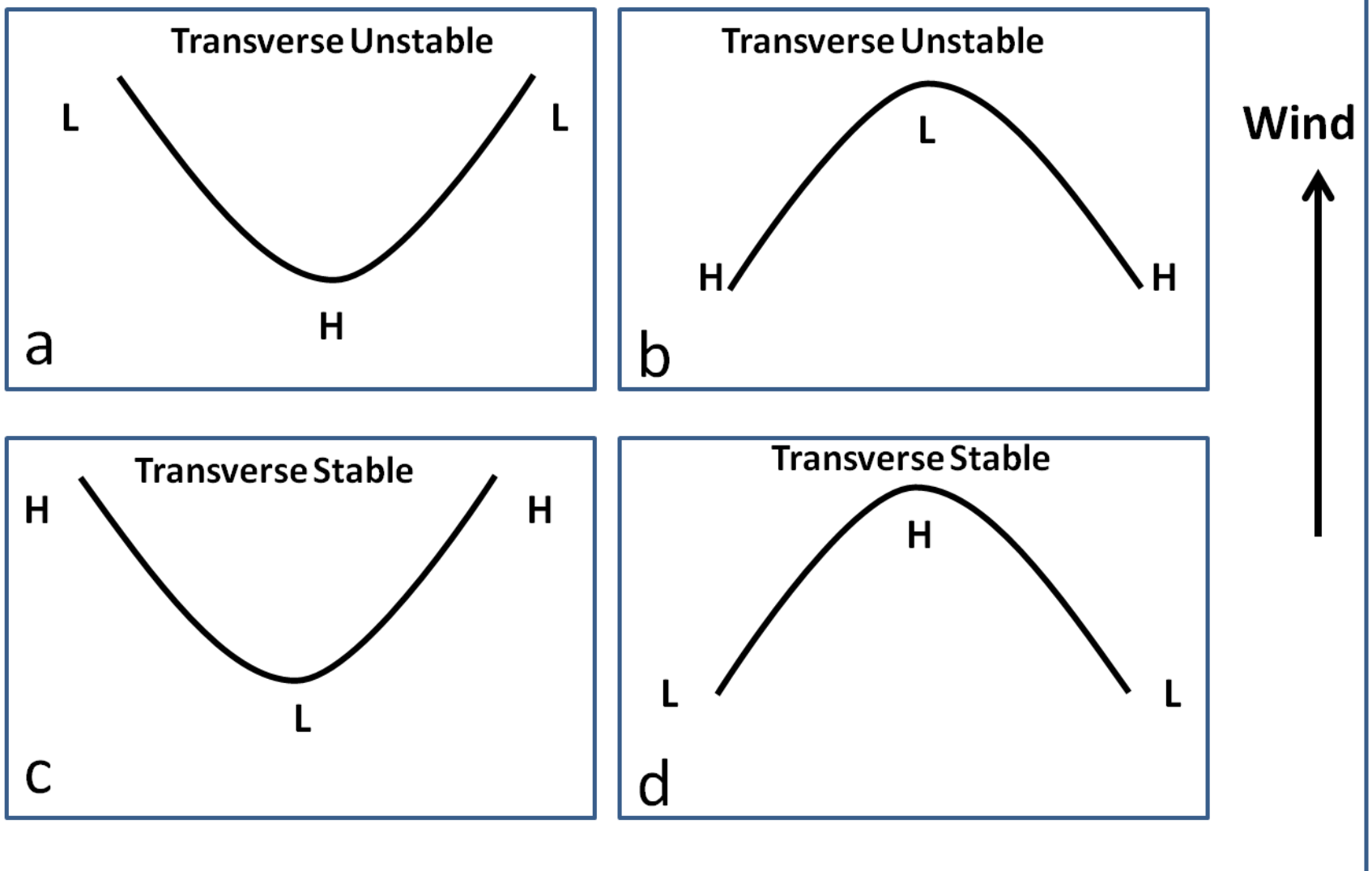

The higher sections are coarser

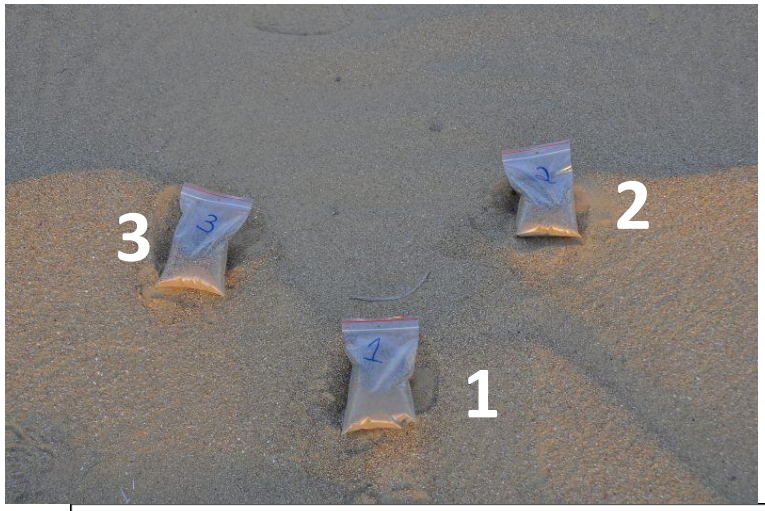

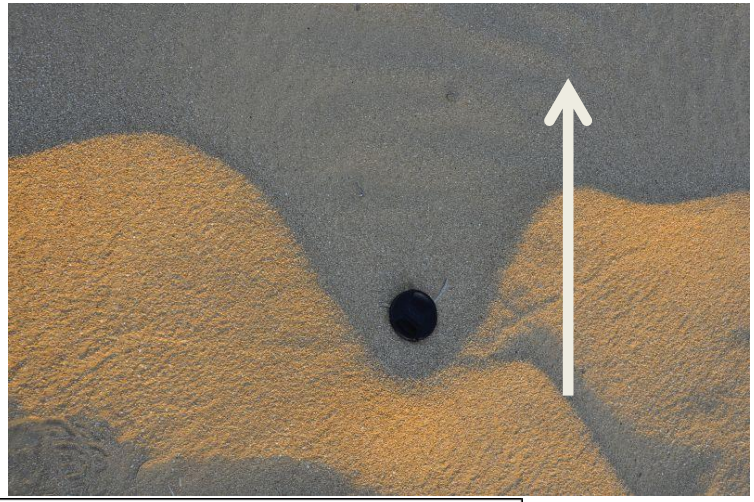

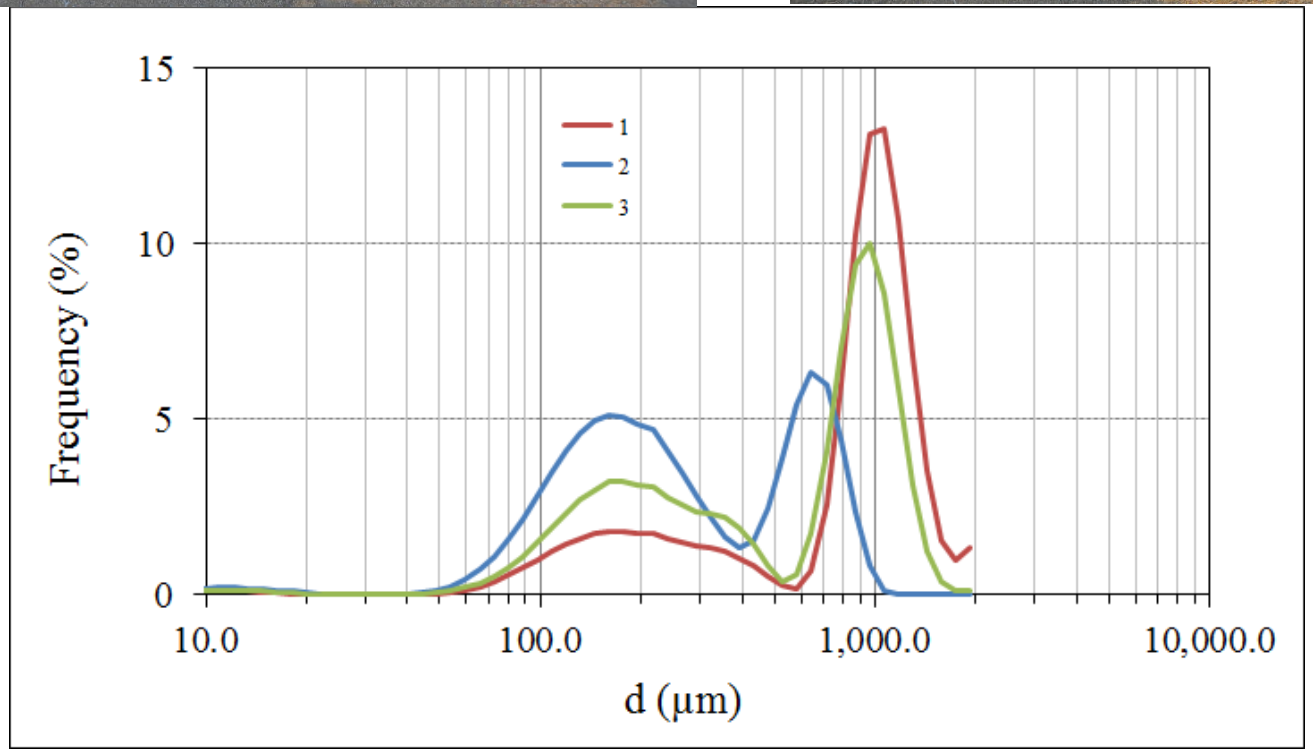

Field measurements

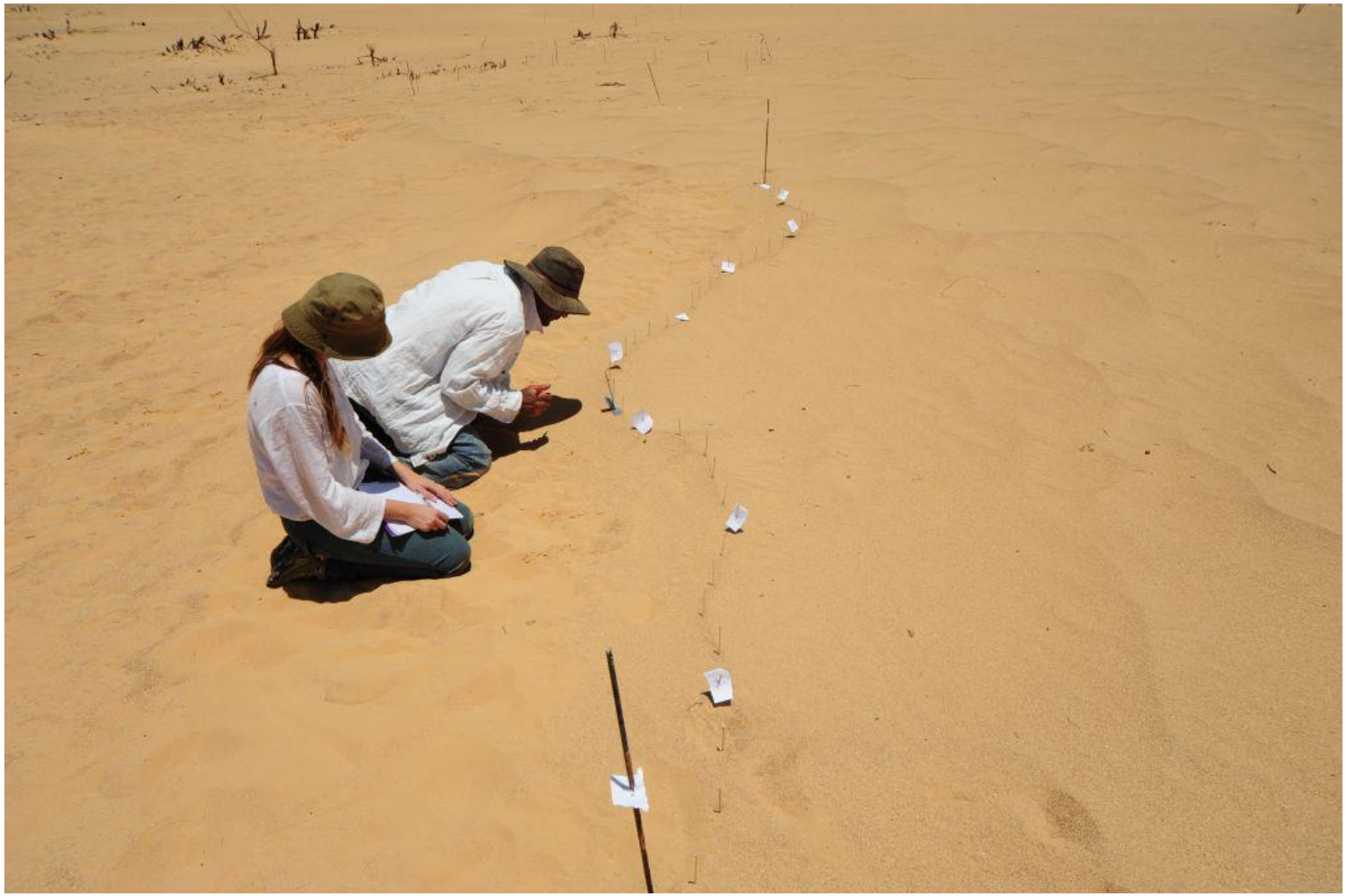

Grain size distribution along the megaripple crest

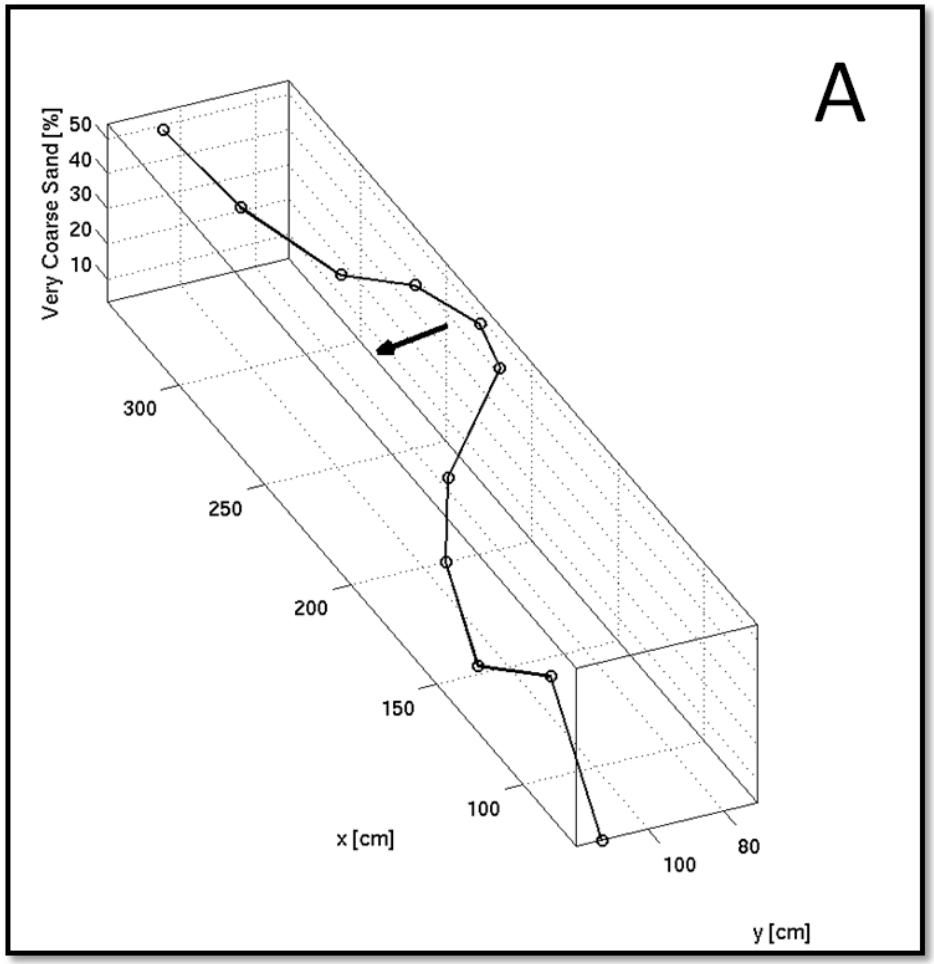

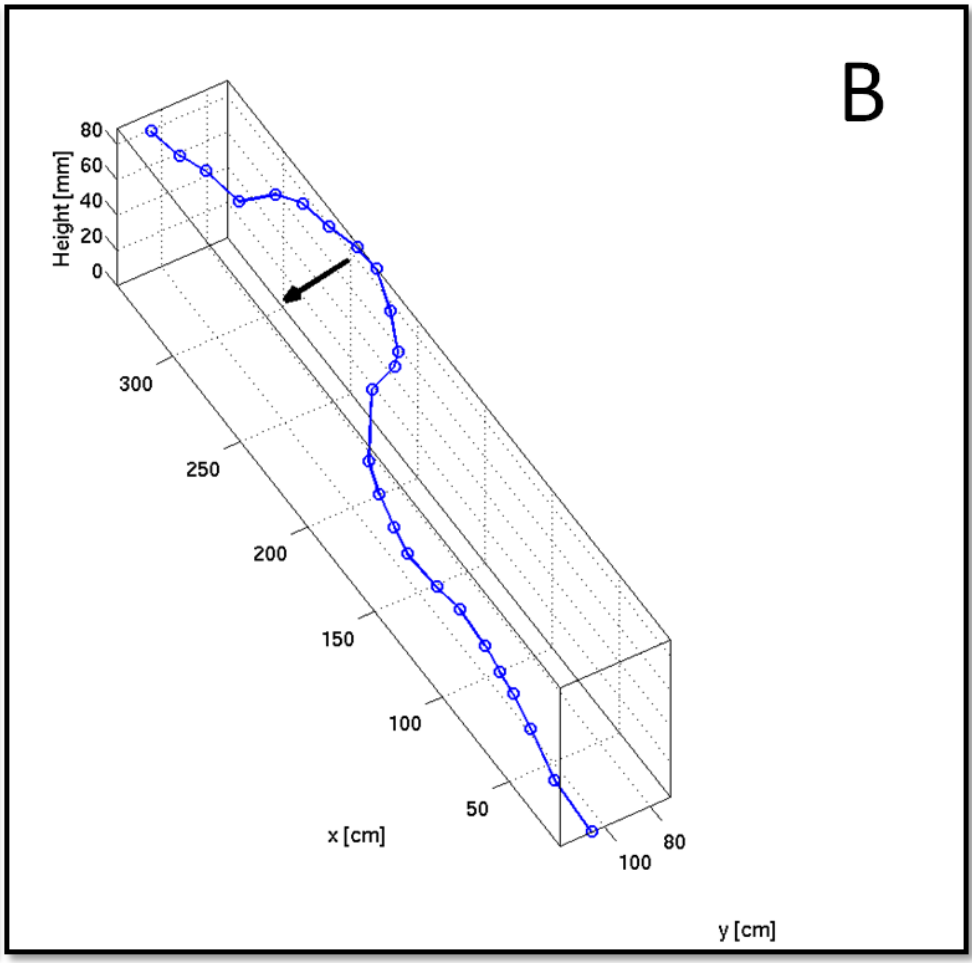

There are different in the armoring layer along the ripple crest

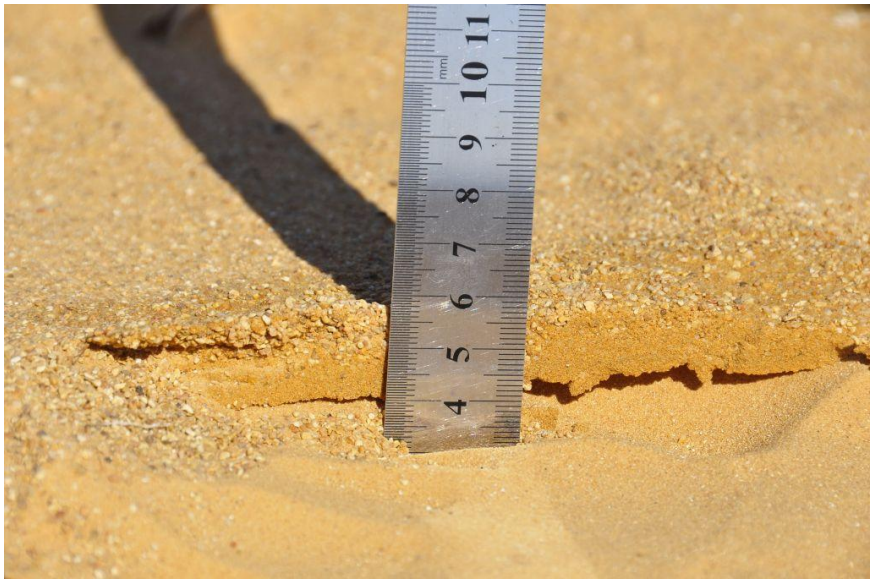

Width=6 mm
at the lowest point of the megaripple

Width=10 mm
at the highest point of the megaripple

The highest part along the megaripples are coarser

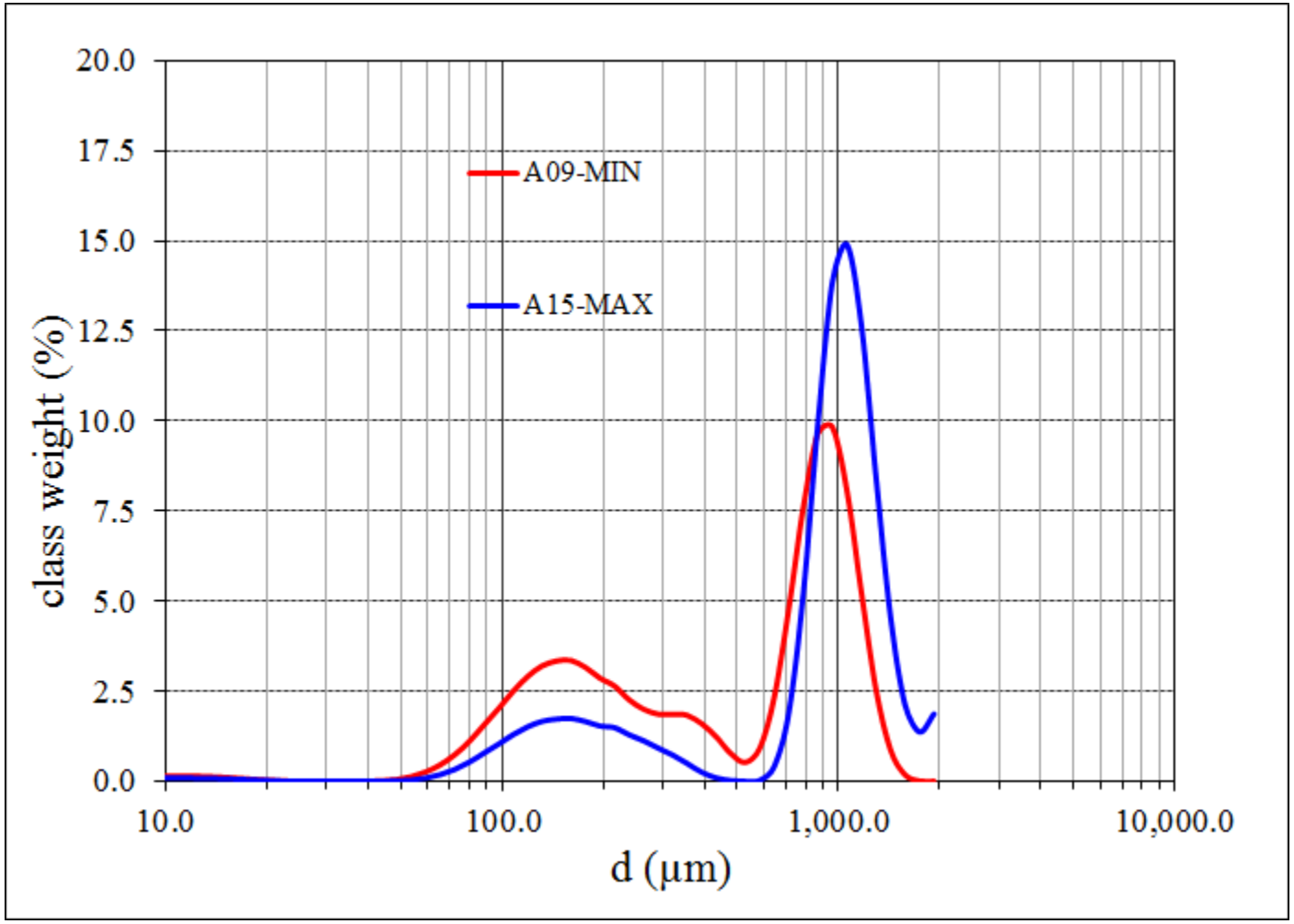

More results from other megaripples

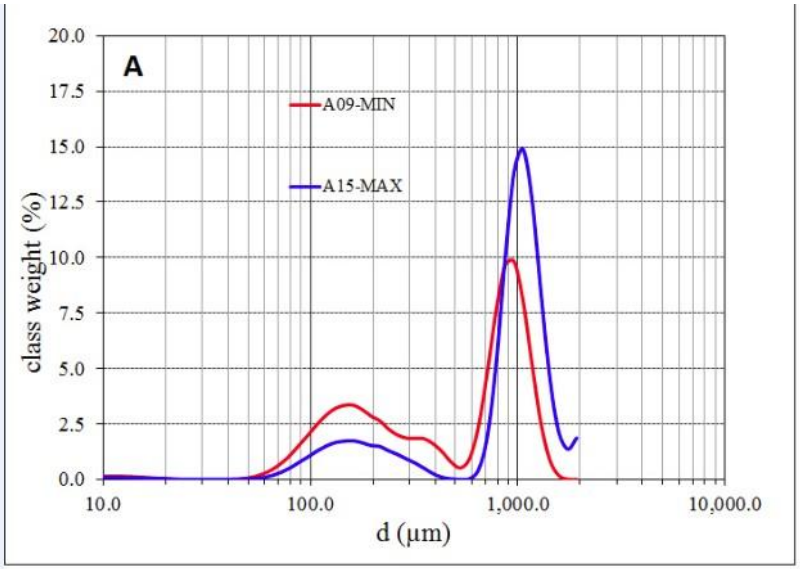

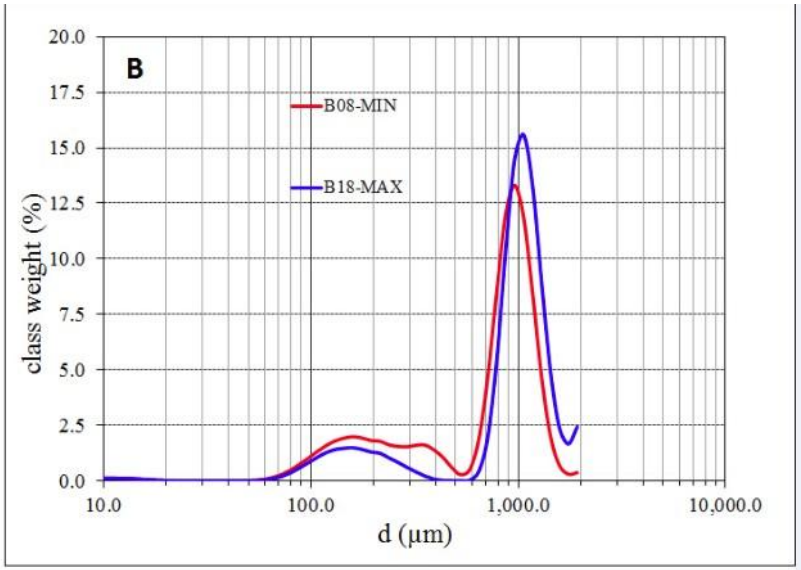

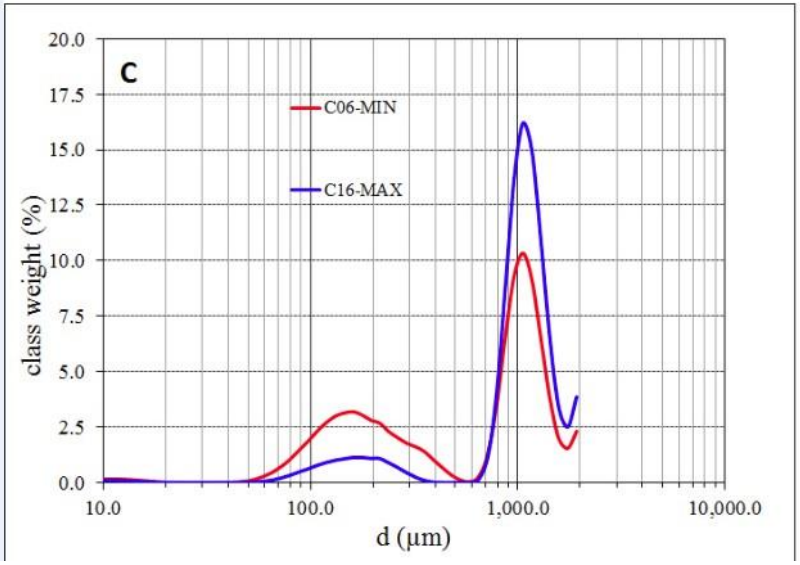

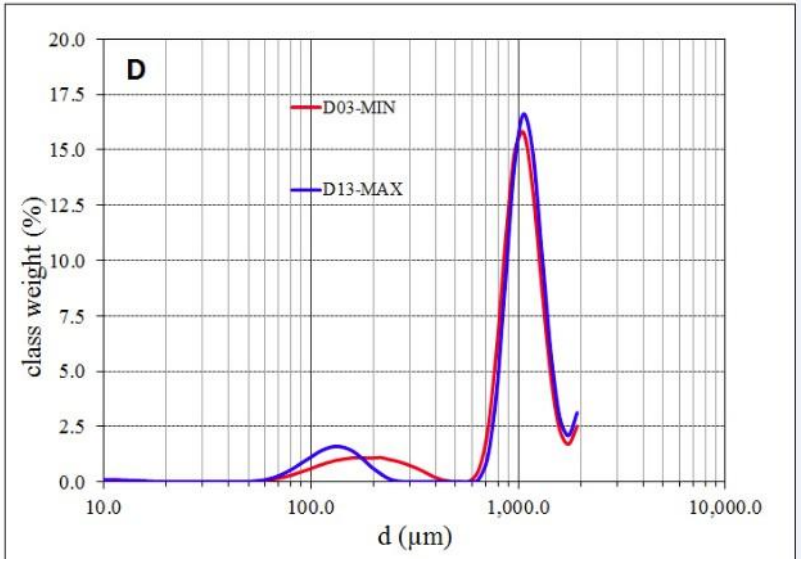

New Indices for bimodal grain size distribution

$$\beta_1 = \frac{D_c - D_f}{D_c}, \quad 0 < \beta_1 < 1$$

Size segregation

$$\beta_2 = \frac{f_c - f_f}{f_c}, \quad -1 < \beta_1 < 1$$

Frequency segregation

c - coarse
f - fine
D –grain diameter
f- frequency


a

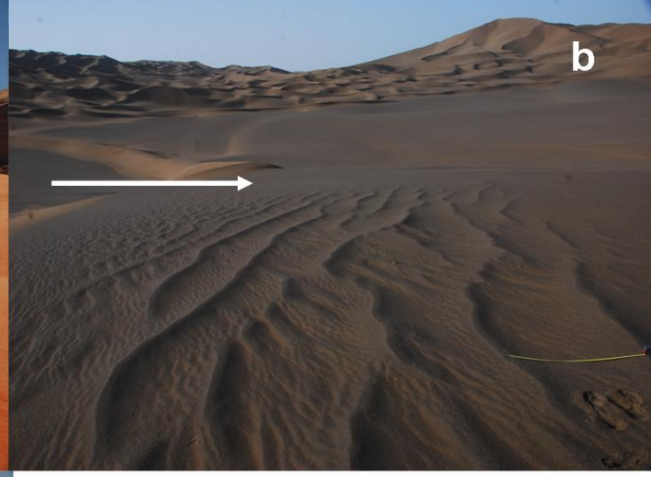
b


c

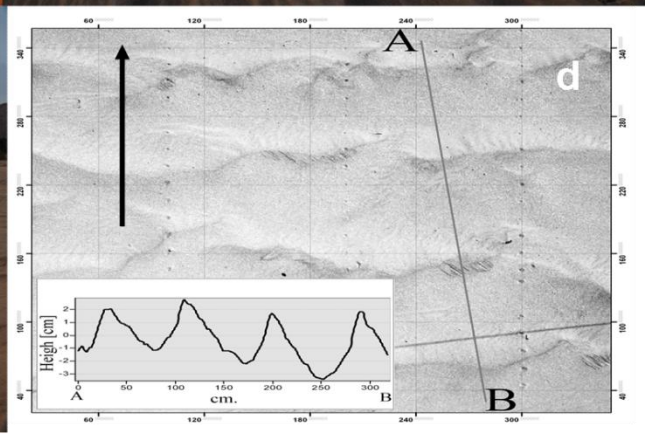
d
A
B
Heigh [cm]
cm.

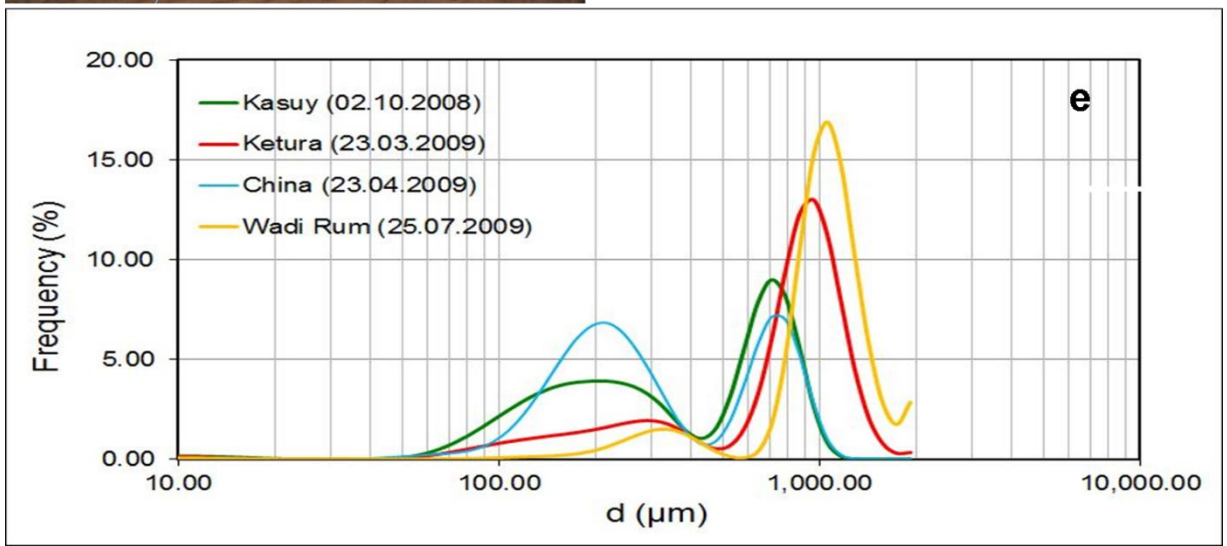
e
Kasuy (02.10.2008)
Ketura (23.03.2009)
China (23.04.2009)
Wadi Rum (25.07.2009)
Frequency (%)
d (μm)
20.00
15.00
10.00
5.00
0.00
10.00
100.00
1,000.00
10,000.00

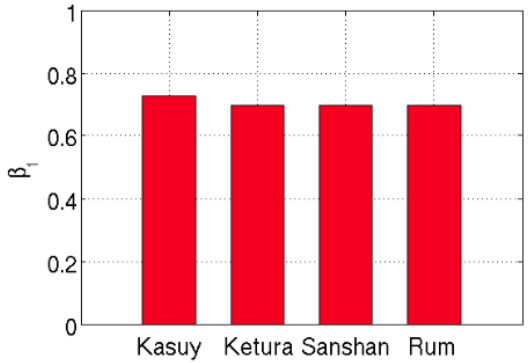
β1
1
0.8
0.6
0.4
0.2
0
Kasuy
Ketura
Sanshan
Rum

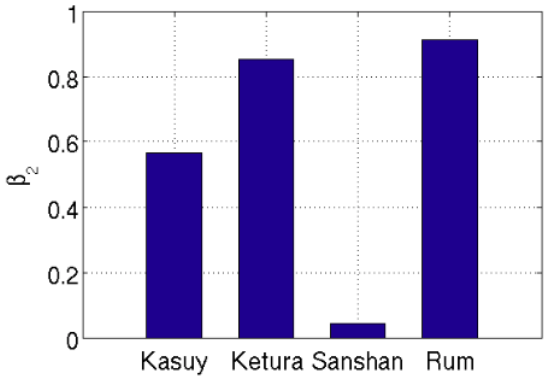
β2
1
0.8
0.6
0.4
0.2
0
Kasuy
Ketura
Sanshan
Rum

Results for 4 megaripples

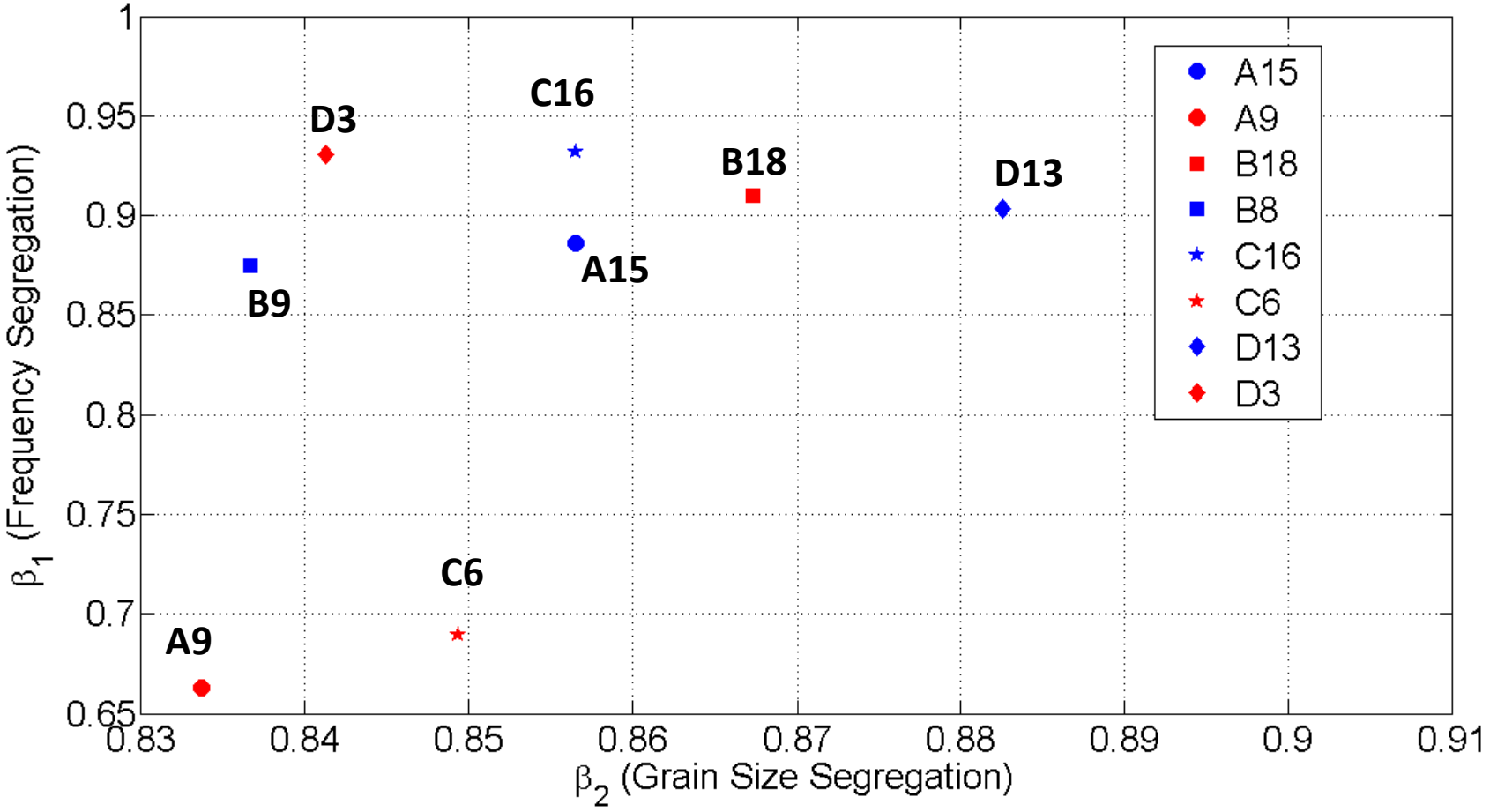

Results from Wadi Rum – Jordan

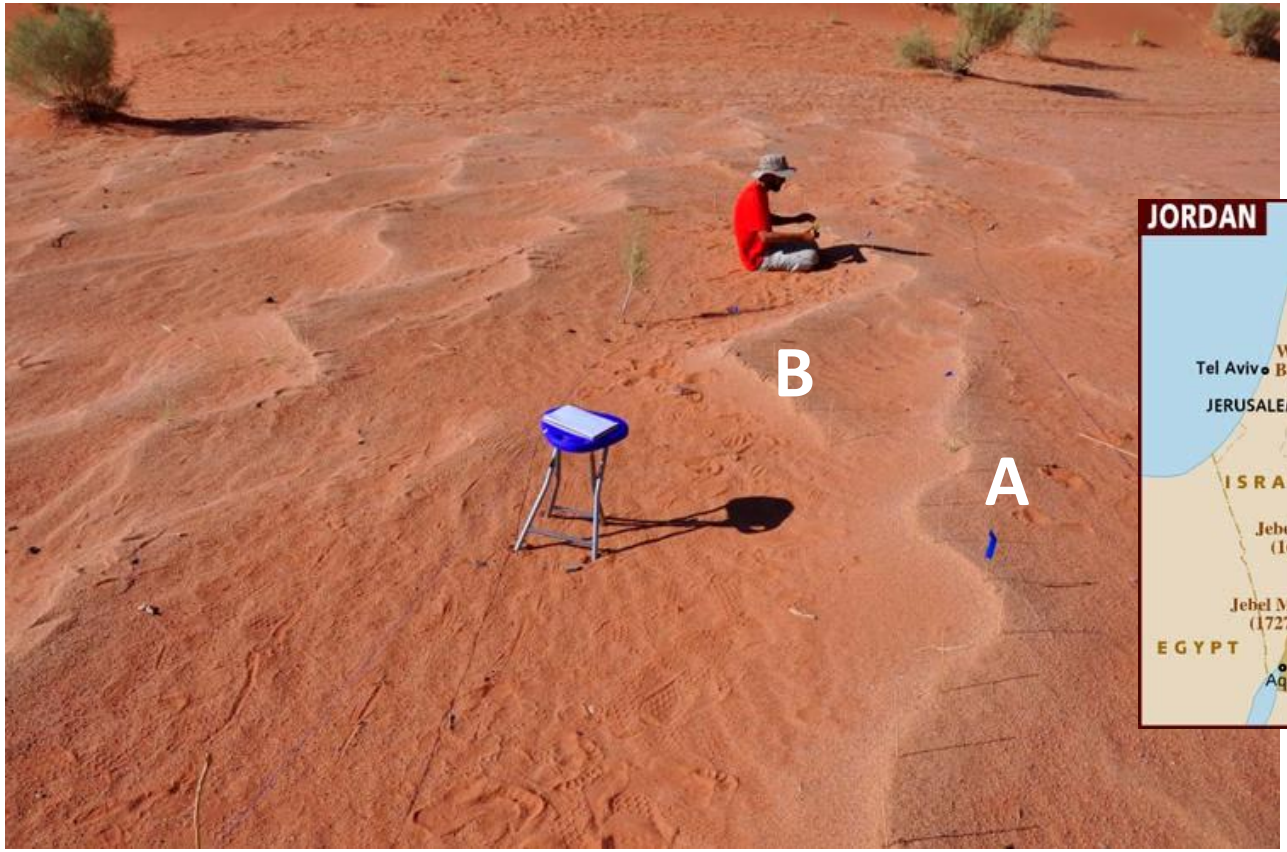

$$SI = \frac{l}{L}$$

Measure of the megaripple sinuosity
l actual length along the crest
L shortest length

$$SI(A) = 7.2 / 6.3 = 1.19$$

$$SI(B) = 7.2 / 6.6 = 1.09$$

Grain-size distribution along the crest (30 cm intervals)

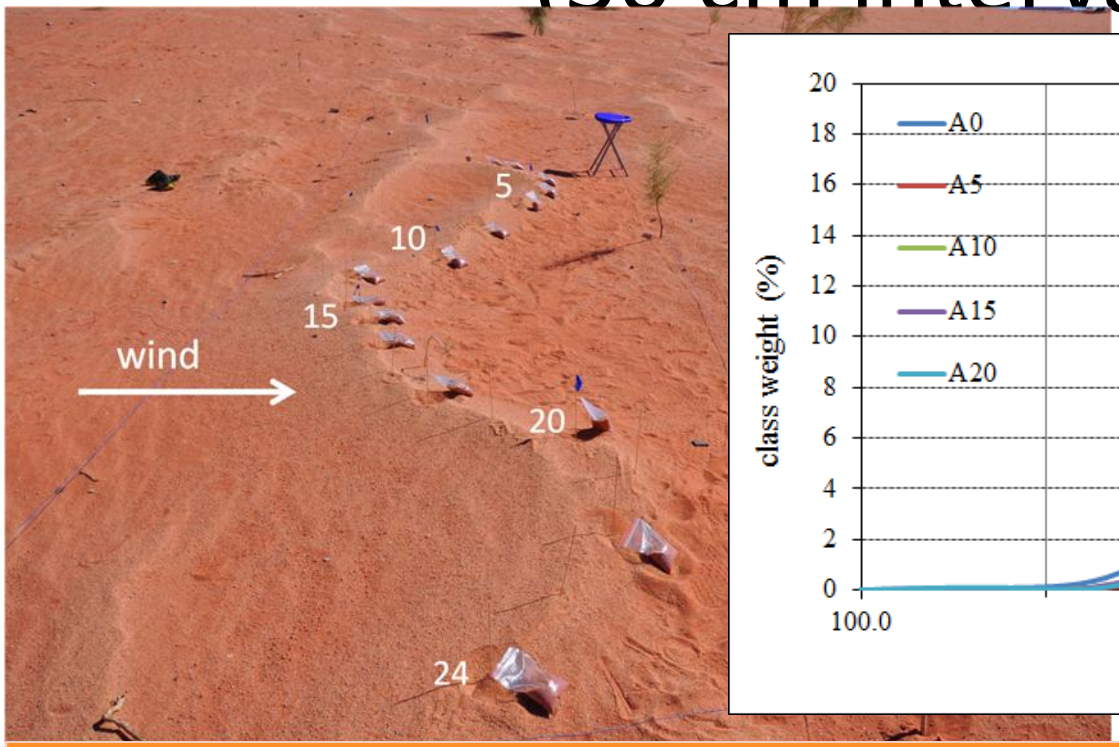

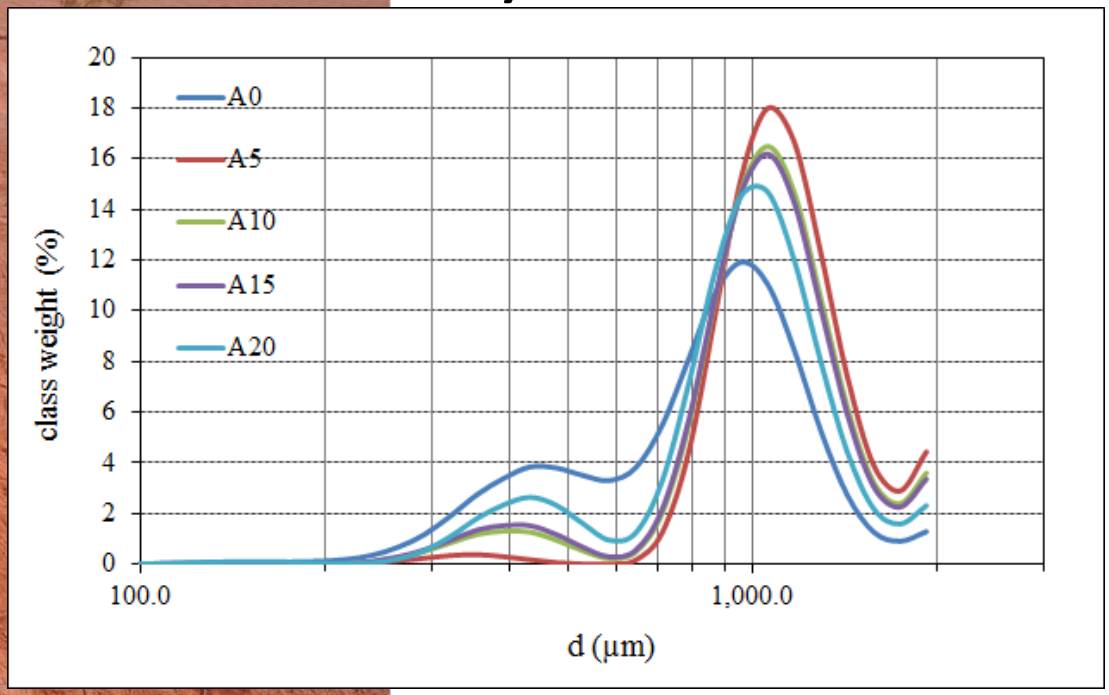

Wadi Ram Jul 2013	A0	A5	A10	A15	A20
Coarse Mode	959	1060	1060	1060	1060
Fine Mode	433	355	392	392	433
Frequency Coarse	11.92	18	16.49	16.09	14.69
Frequency Fine	3.58	0.39	1.31	1.53	2.94
Minimum F	3.31	0	0.24	0.3	0.96
Minimum D	584	584	584	584	584

possible scenario for development of the transverse instability.

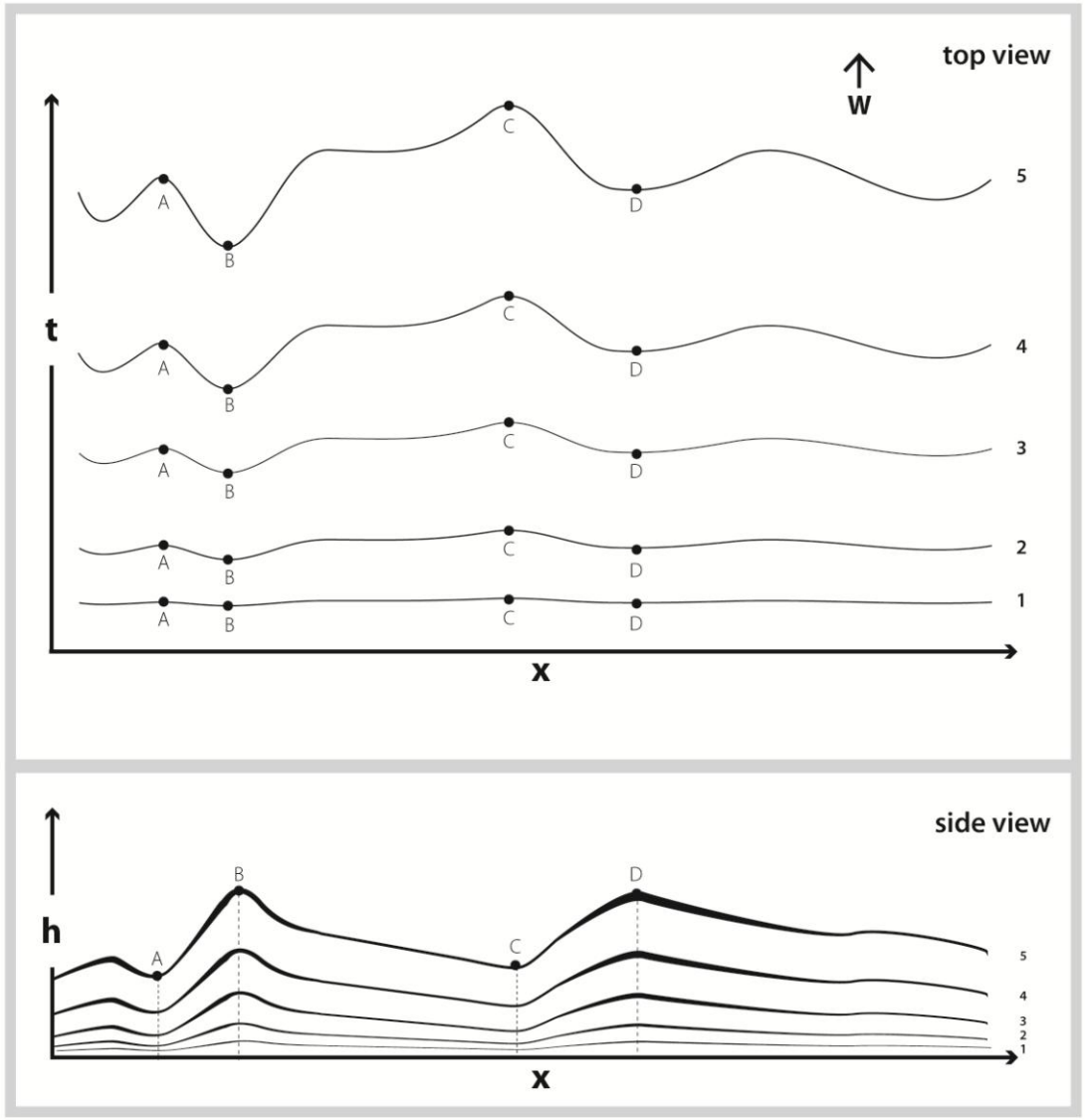

Megaripples on Mars

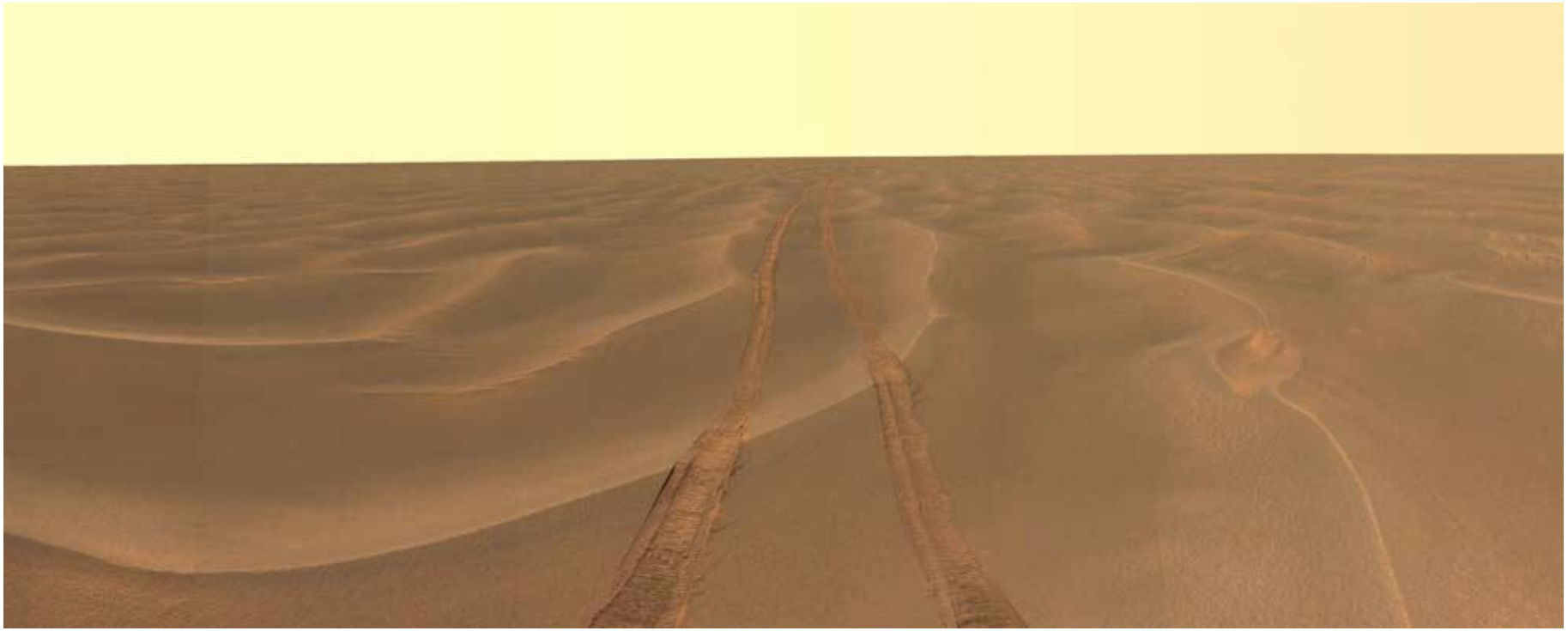

Approximate true color Pancam panorama of eolian ripples on the Meridiani plains (Squyres et al., 2006)

What are the TARs (Transverse Aeolian Ridges)? Small dunes, Large ripples or Megaripples

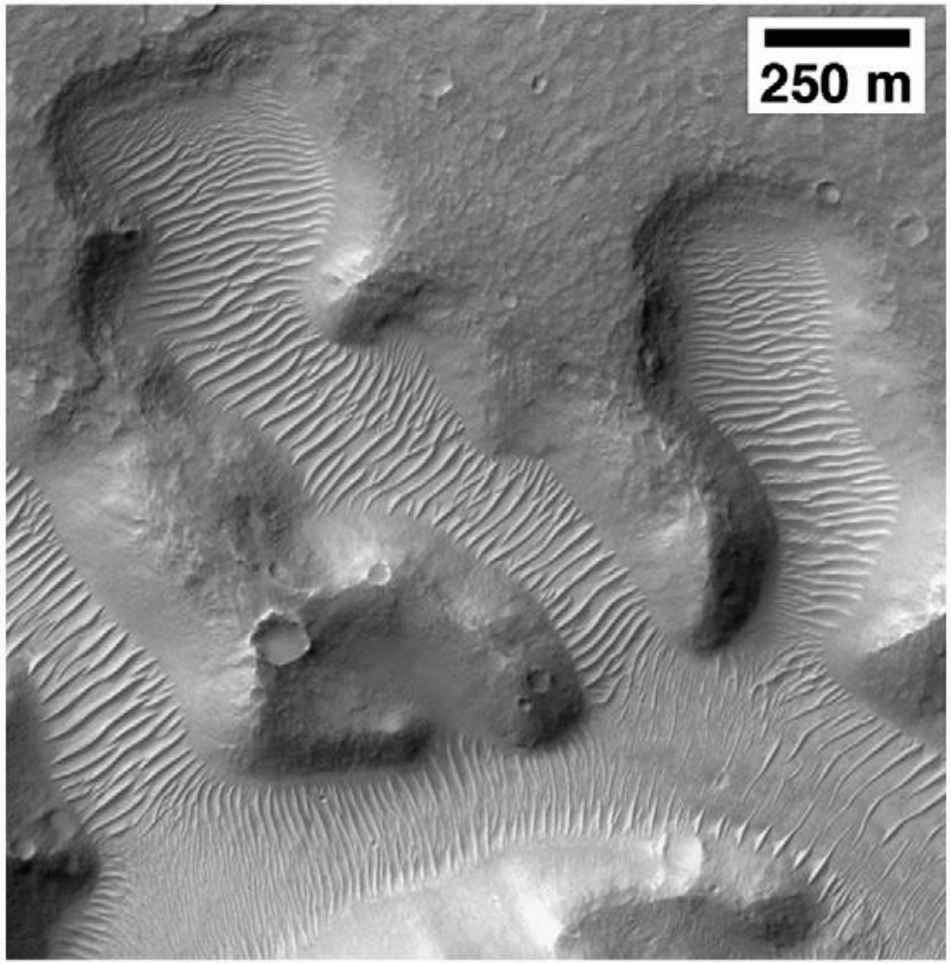

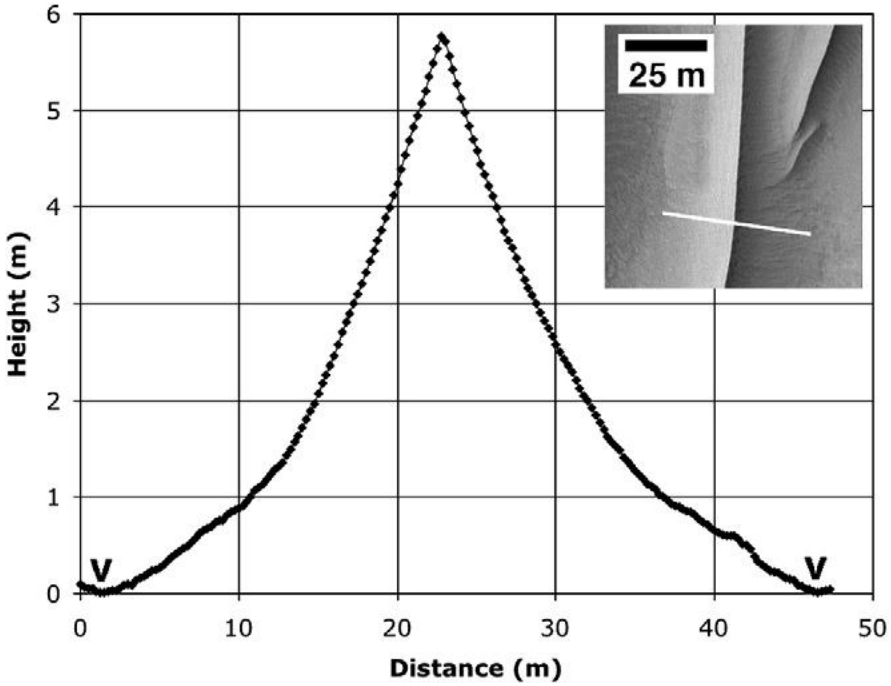

Zimbelman, 2010

Can the sinuosity of the bedforms can help to identify them?

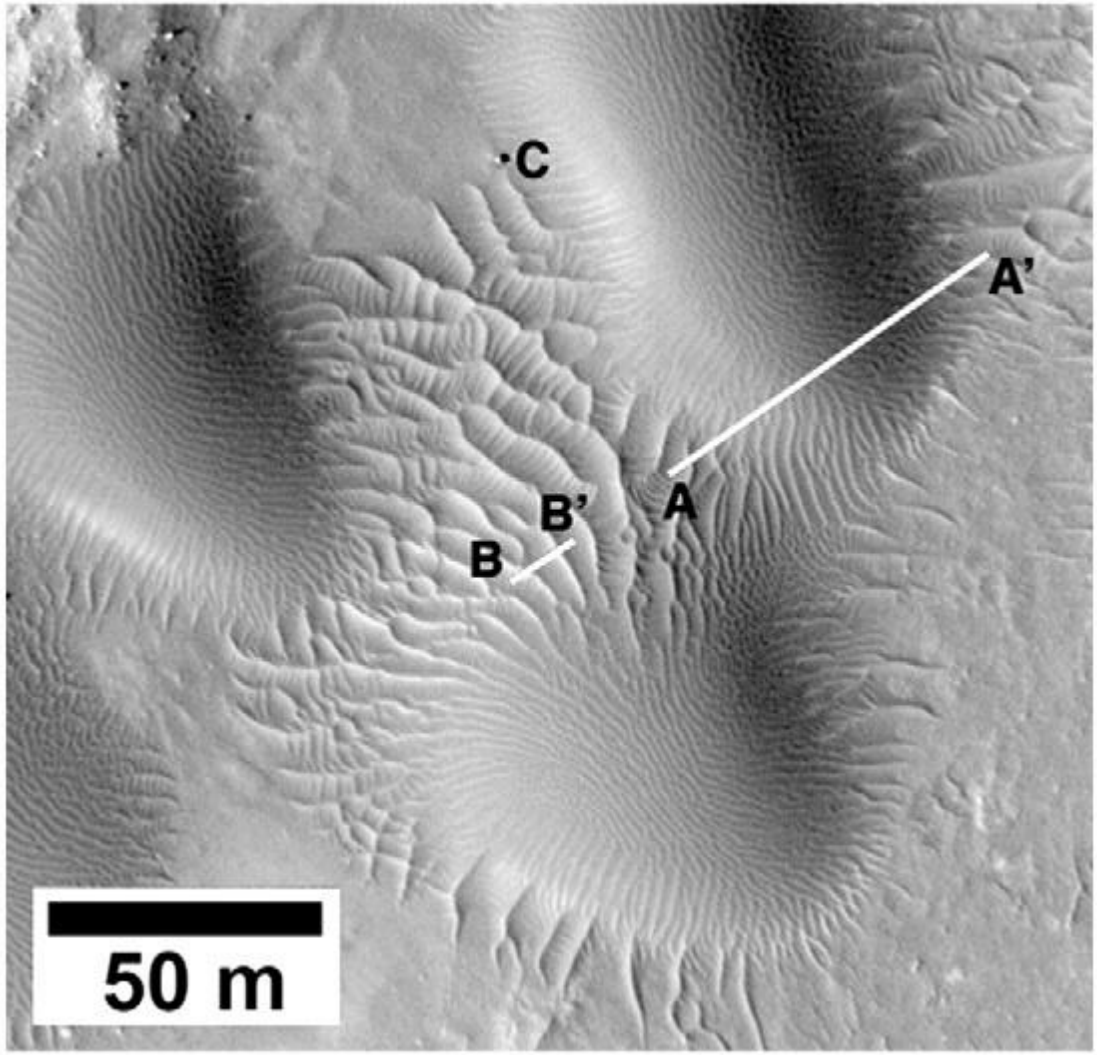

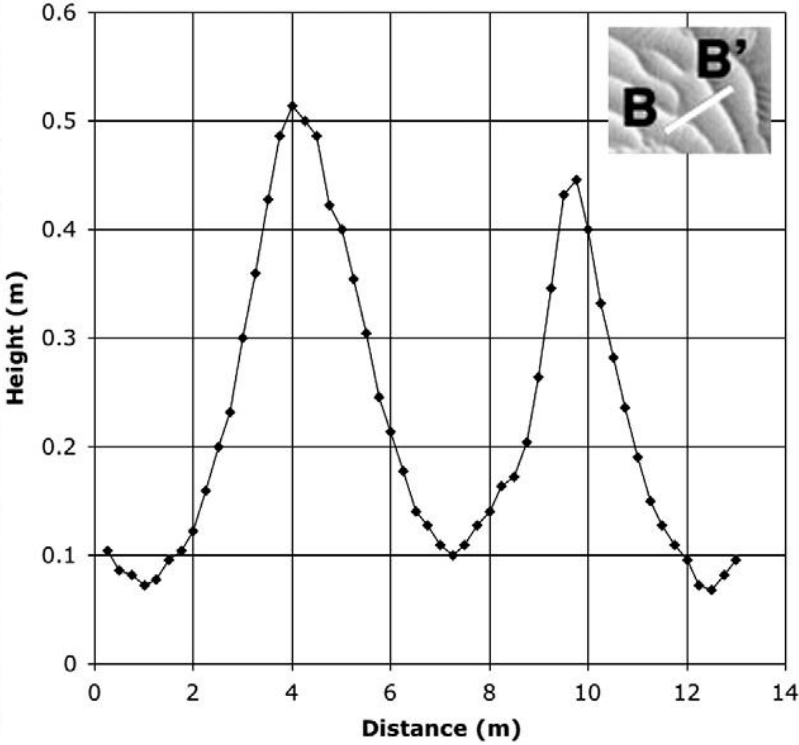

Summary

- Sand ripples are transverse stable whereas megaripples are transverse unstable.
- There is a size segeration along the crest of the megaripples, the highest places are coarser.
- The thickness of the armoring layer along the megaripples crest is non uniform; it is larger at the higher sections of the ripple.
- The lateral coupling in megaripples is smaller than in normal ripples- the reptation flux is smaller in the lateral direction than in the wind direction.

Future Studies

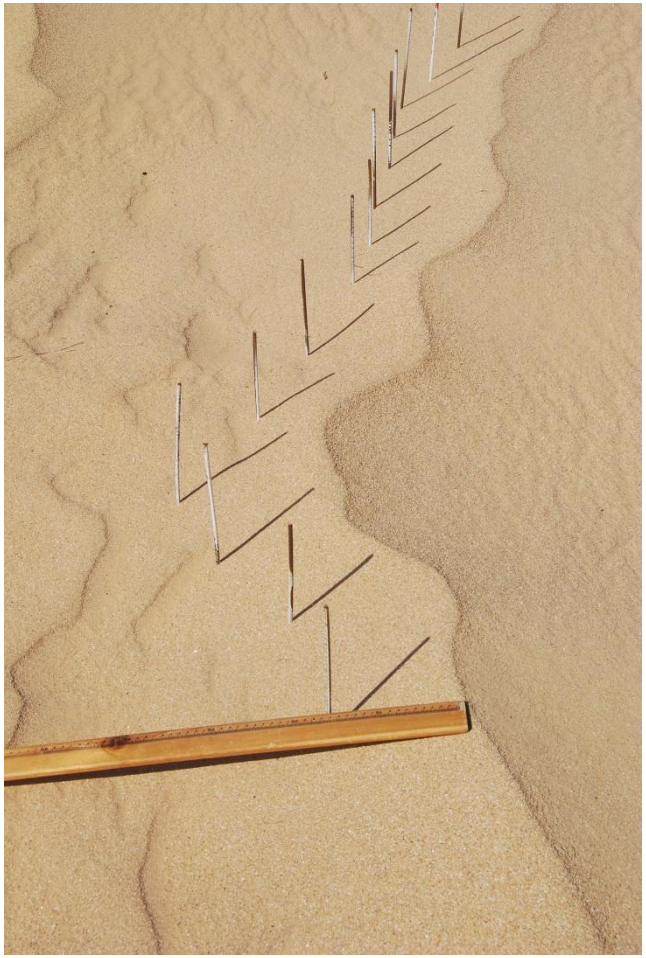

- Studying the spatiotemporal dynamics of a field of megaripples and the relation between the different crest.
- What is the mechanism that prevents segmentation of the crests?
- Mathematical model for megaripples (3D?)

3D study of the splash distribution for different grain size distribution

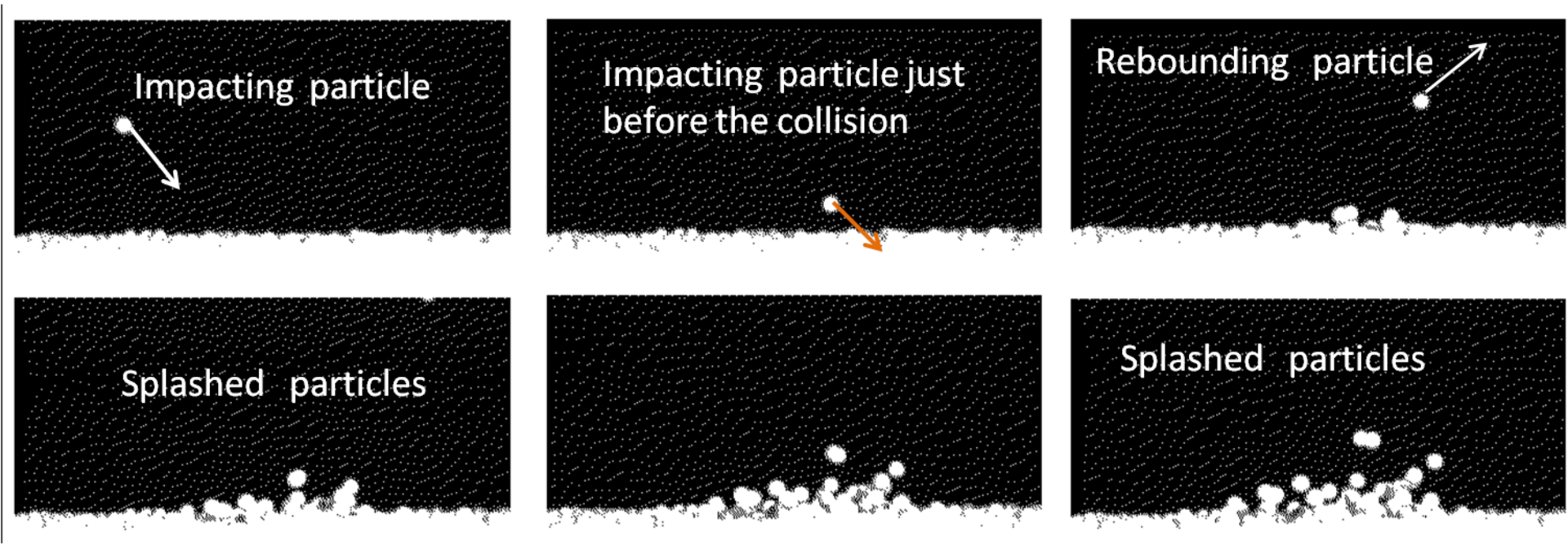

Beladjine et al. 2007

Relevant Papers

Anderson, R.S., 1987. A theoretical model for impact ripples. *Sedimentology*, 34, 943-956.

Anderson, R.S. and Haff, P.K., 1988. Simulation of eolian saltation. Science, 241, 820-823.

Anderson, R.S. 1990. Eolian ripples as example of self-organization in geomorphological systems. *Earth-Science Reviews*, 29, 77-96.

Andreotti, B., 2004. A two-species model of aeolian sand transport, *J. Fluid Mech.*, 510, 47-70.

Bagnold R.A., 1941. The Physics of Blown Sand and Desert Dunes. Methuen, London.

Balme, M., Berman, D. C., Bourke, M. C. and Zimbelman, J. R., 2008. Transverse Aeolian Ridges (TARs) on Mars. Geomorphology, 101, 703-720.

Beladjine, D., Ammi, M., Oger, L. and Valance, A. 2007. Collision process between an incident bead and a three-dimensional granular packing. Phys. Rev. E 75 061305.

Gordon, M. and Neuman, C. M., 2011. A study of particle splash on developing ripple forms for two bed materials. *Geomorphology*, 129, 79–91.

Kok, J. F. and Renno, N. O., 2009. A comprehensive numerical model of steady state saltation (COMSALT). *Journal of Geophysical Research*, 114, D17204.

Manukyan, E. and Prigozhin, L. 2009. Formation of aeolian ripples and sand sorting. *Phys. Rev. E*, v. 79, art. no. 031303.

Yizhaq, H., Balmforth, N.J and Provenzale, A. 2004. Blown by wind: Nonlinear dynamics of aeolian sand ripples. *Physica D*, 195, 207-228.

Yizhaq, H., Katra, I., Kok, J. F. and Isenberg, O., 2012. Transverse instability of megaripples.

Zimbelman, J.R. 2010. Transverse Aeolian Ridges on Mars: First results from HiRISE images, *Geomorphology, 121*, 22-29, doi: 10.1016/j.geomorph.2009.05.012, 2010.

Geology, 40, 459-462.